Electronic structure determination using HAXPES: current activity and future perspectives at DESY

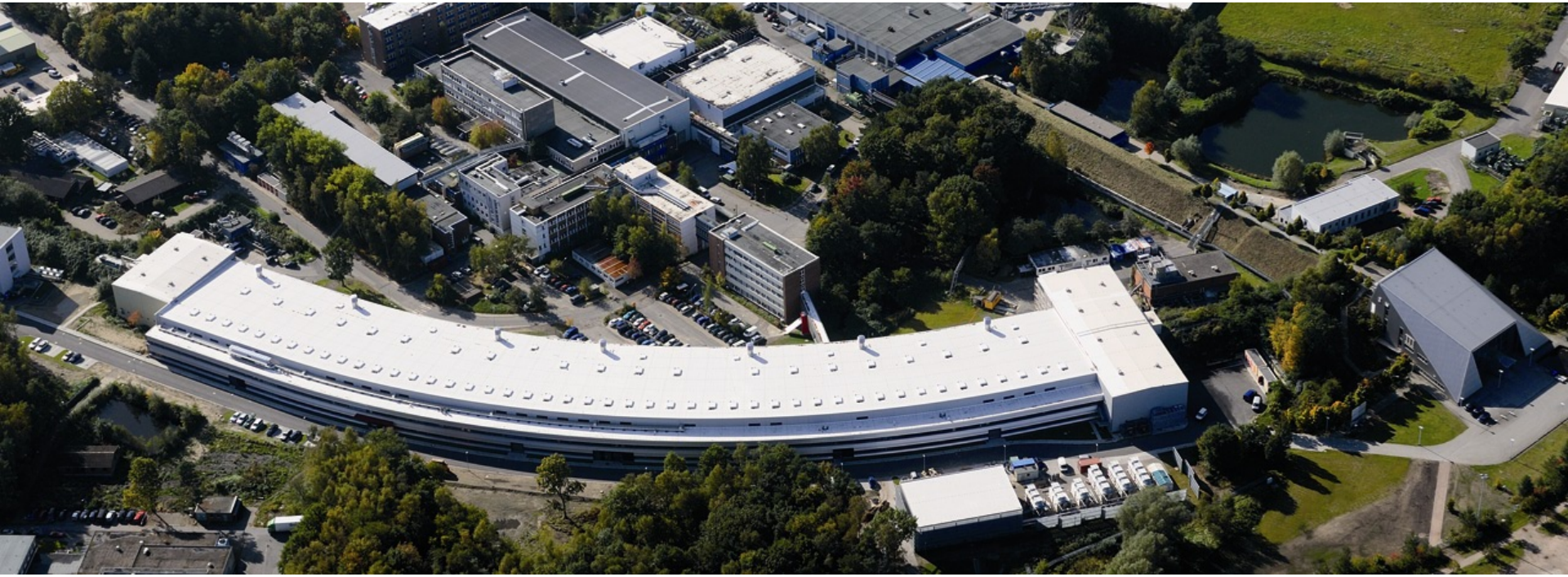

HELMHOLTZ
GEMEINSCHAFT

Wolfgang Drube

HAXPES Workshop
NSLS May 20-22, 2009

DESY

Why „hard“ X-rays (hν ~ 2-15 keV) ?

Main advantages:

- "true" bulk sensitivity (on a few nm scale, typ. 10 nm)
- not surface-sensitive → no *(in situ)* surface preparation required
- study of *"as is"* samples (thin films, device physics, ...)
- scattering easier to handle in the analysis
- short wavelength → generate Bragg reflections (single crystals)

Applications in *basic physics* and *applied materials science*:

- volume electronic structure of complex materials
- buried interfaces and nano-structures
- tunability of surface vs. bulk sensitivity (depth profiling)
- resonant inner-shell excitations
- X-ray standing waves: electronic ←→ geometric structure
- ...

Why „hard“ X-rays ($h\nu \sim$ 2-15 keV) ?

Drawbacks:

- limited (if any) k-resolution, recoil effects
- cross section $\sim h\nu^{-(2...4)}$ (depending on subshell) + non-dipole
- need for high photon flux (and brilliance)
- electron analyzer transmission $\sim E_{kin}^{-1}$
- need for stable HV electron analyzers + efficient low noise detectors (now available)

Applications in *basic physics* and *applied materials science*:

- volume electronic structure of complex materials
- buried interfaces and nano-structures
- tunability of surface vs. bulk sensitivity (depth profiling)
- resonant inner-shell excitations
- X-ray standing waves: electronic ←→ geometric structure
- ...

Current HAXPES instruments worldwide

List may incomplete (please complain afterwards)

SPring-8:

BL15XU (National Institute for Materials Science (NIMS)
WEBRAM (Wide Energy Beamline for Research in Advanced Materials)
coll. with Hiroshima university
BL19LXU temporary (Osaka university)
BL29XU RIKEN Coherent X-ray Optics (temporary)
BL46XU Engineering science research III
Hard X-ray Photoemission Spectroscopy JASRI
BL47XU (HXPES·MCT) JASRI

ESRF:

ID16 inelastic scattering (VOLPE, temporary)
ID32 permanent instrument
BM25 SpLine HV-CSA , HAXPES+SXRD (permanent)

BESSY II:

KMC-1 (bending magnet) HIKE, permanent instrument

NSLS:

X24A (bending magnet) 1.8 - 6 keV (permanent instrument)

DESY:

BW2 (wiggler) permanent instrument

Energy dependence of inelastic mean free path

excitation energy → λ_{IMFP}

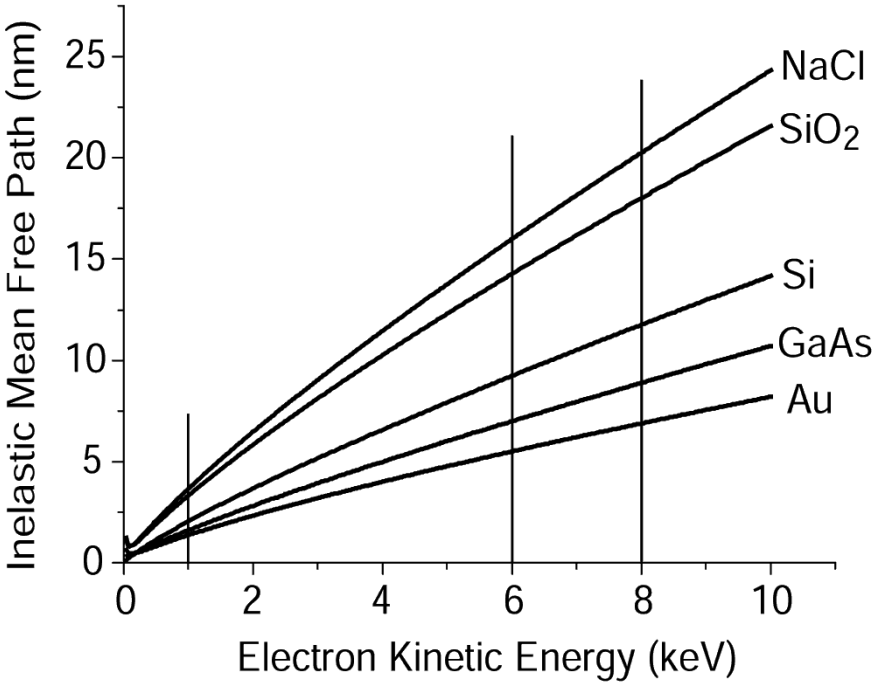

Y. Takata et al.
(NIST database)

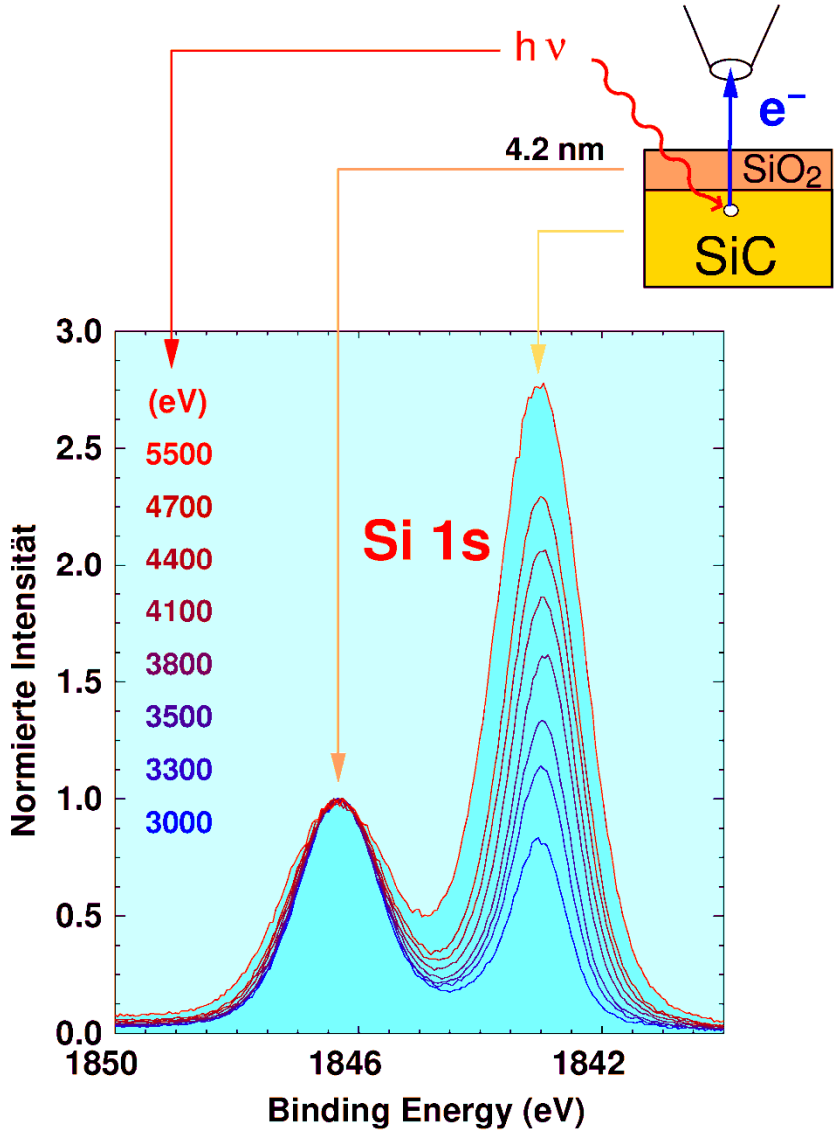

Surface / bulk sensitivity

ISO 18115:2001 Surface chemical analysis: vocabulary (buy for 158 CHF)

brief overview: Powell&Jablonski, NIM A601, 54 (2009)

IMFP – inelastic mean freen path
a materials property
calc. from optical data or elastic electron back scattering
predictive IMFP formula (Tanuma et al., TPP-2M)

EAL – effective attenuation length
takes into account elastic scattering,
used to replace IMFP in suitable formulae

MED – mean escape depth

$$D = \int_0^\infty z\phi(z,\alpha)\,\mathrm{d}z \Big/ \int_0^\infty \phi(z,\alpha)\,\mathrm{d}z$$

ID – information depth
depends strongly on the analysis method

neglect elast. scatt.

$$\Delta = \lambda_i \cos\alpha$$

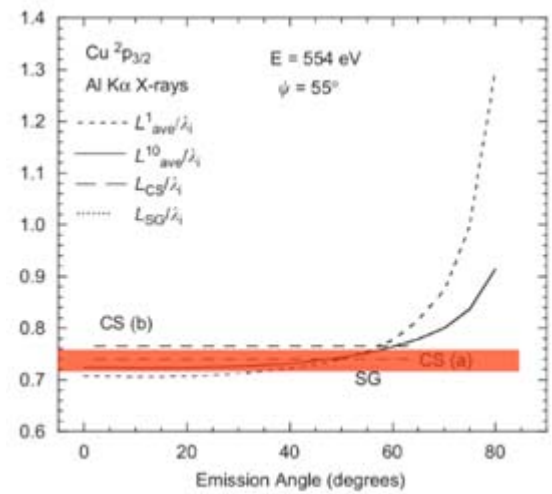

with harder X-ray excitation, the linear models should work better (e.g. increased forward scattering)

Depth profiling: electron mission angle

effective attenuation length EAL, corrects for elastic scattering

SiO_2 / Si

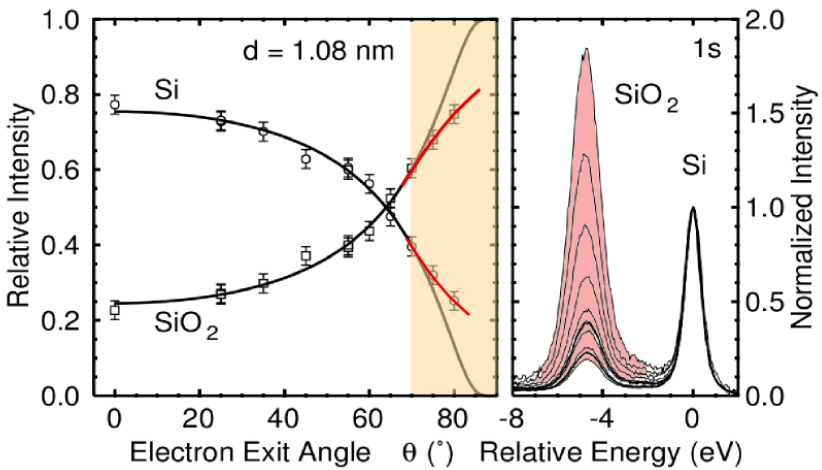

$$I_s = I_s^0 \cdot e^{\frac{-t}{L\cos\Theta}}$$

e.g. overlayer film thickness measurement

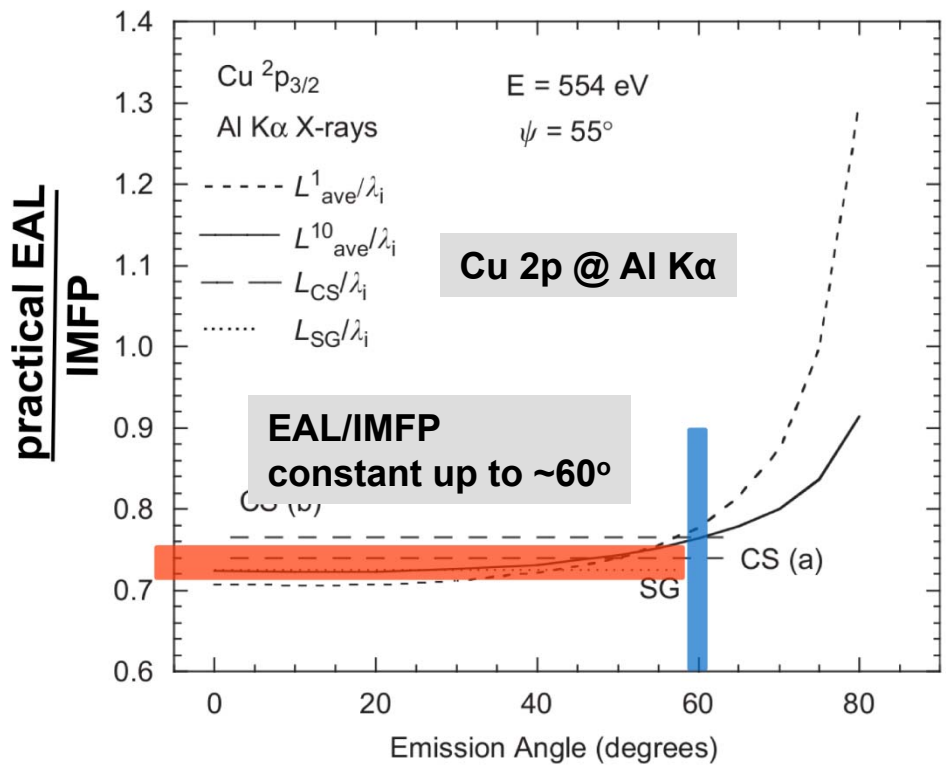

C.J. Powell, A. Jablonski, NIM A601, 54 (2009)

less severe with harder X-ray excitation

Depth profiling: photon incidence angle

$n = 1 - \delta - i\beta$

critical angle $\phi_c \approx \sqrt{2\delta}$

Si (3300 eV):

$\delta = 4.5 \times 10^{-5}$

$\beta = 5.3 \times 10^{-6}$

$\phi_c \approx 10$ mrad (0.57^o)

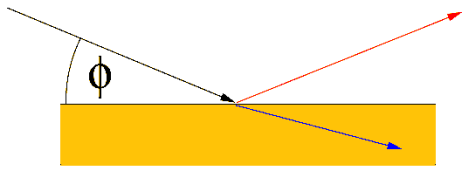

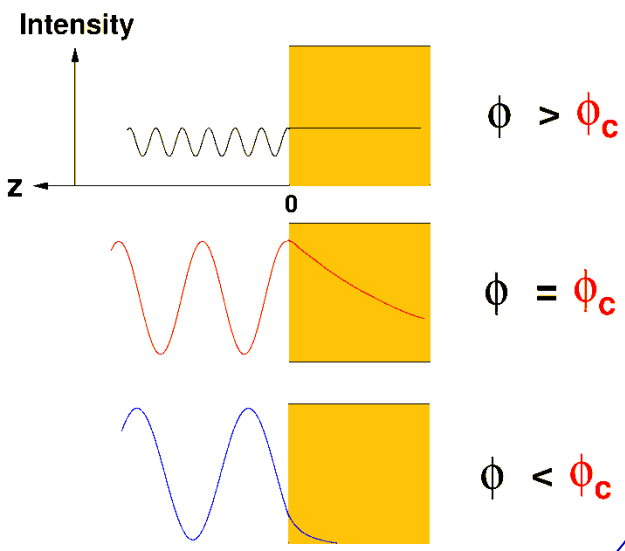

grazing X-ray incidence: total reflexion

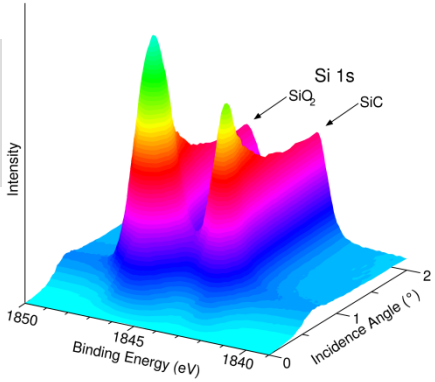

SiO_2 (4.2 nm) / SiC

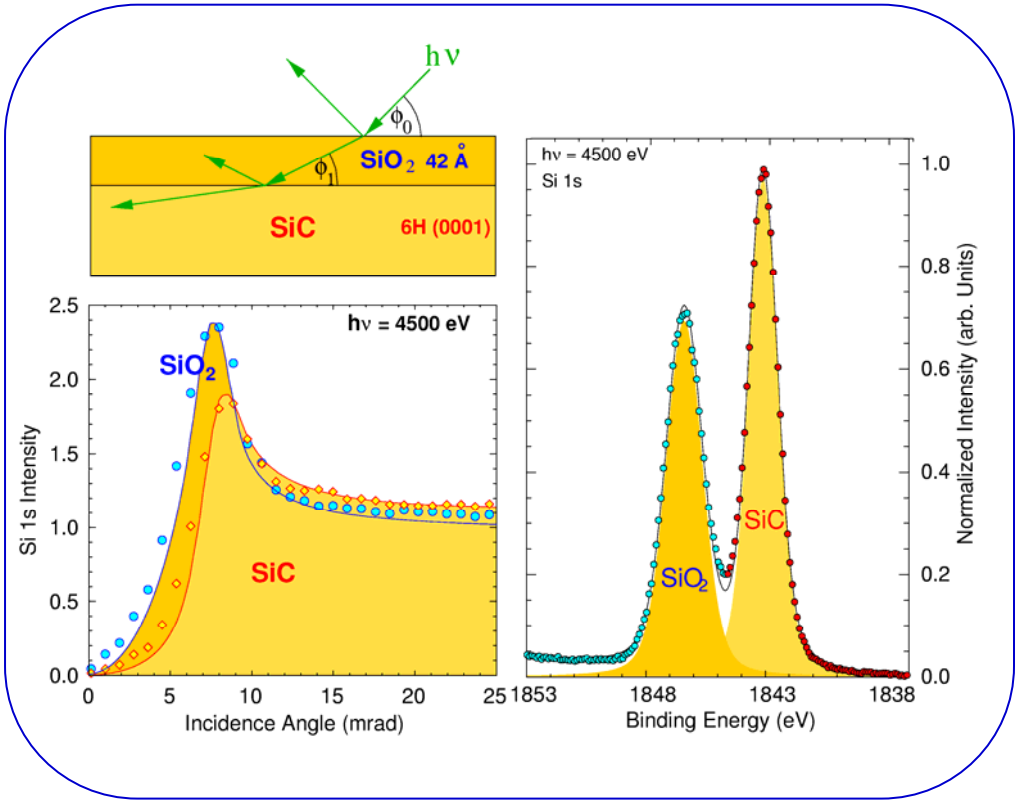

total reflection and XSW

Self-assembling monolayers on Au surfaces

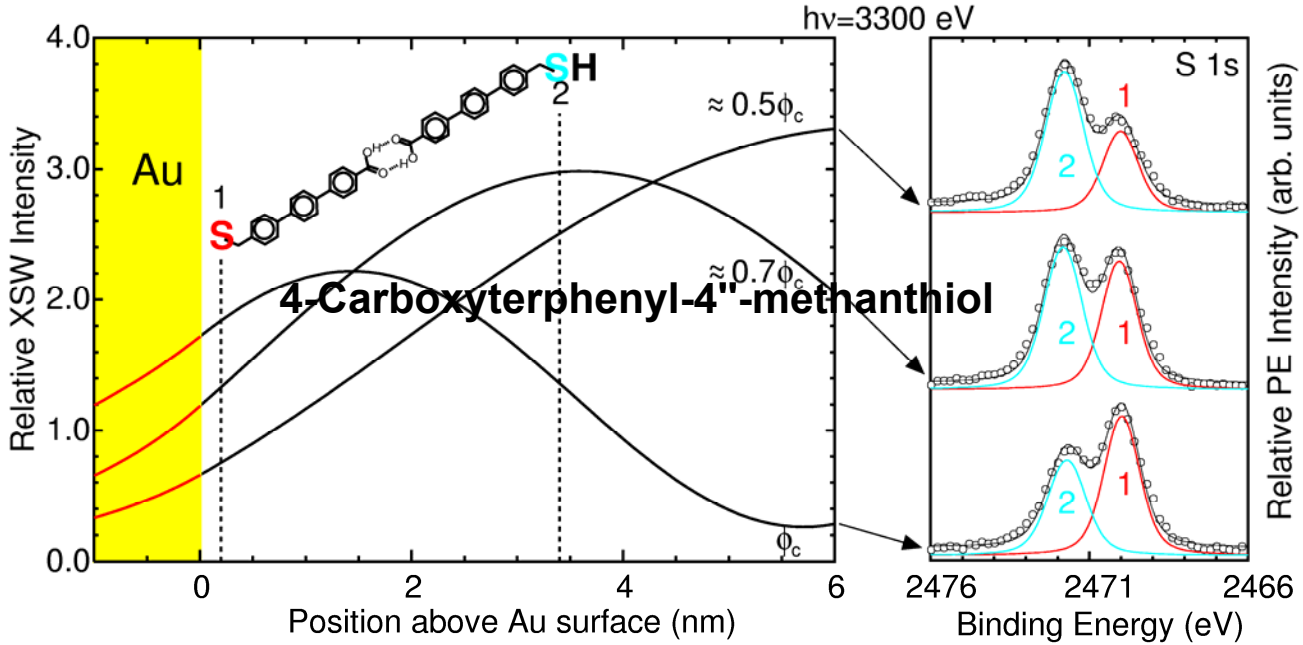

$CH_3(CH_2)_{21}SH$ (C22SH)

radiation induced breakage of molecule
extra S 1s peak

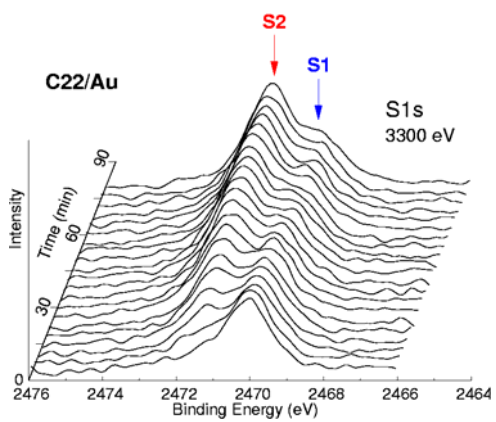

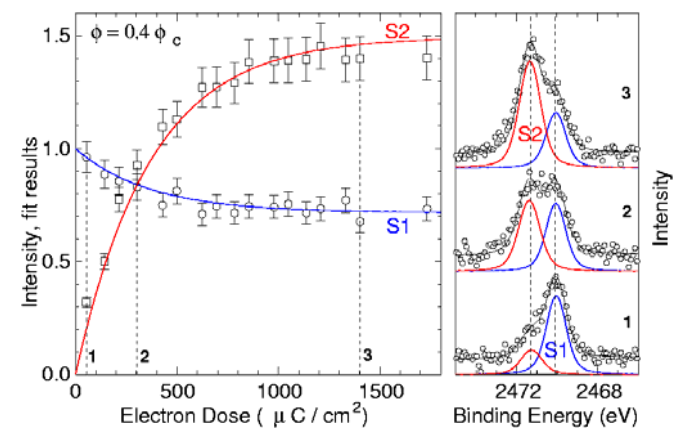

Energy dependence of photoelectric cross section

Scofield:

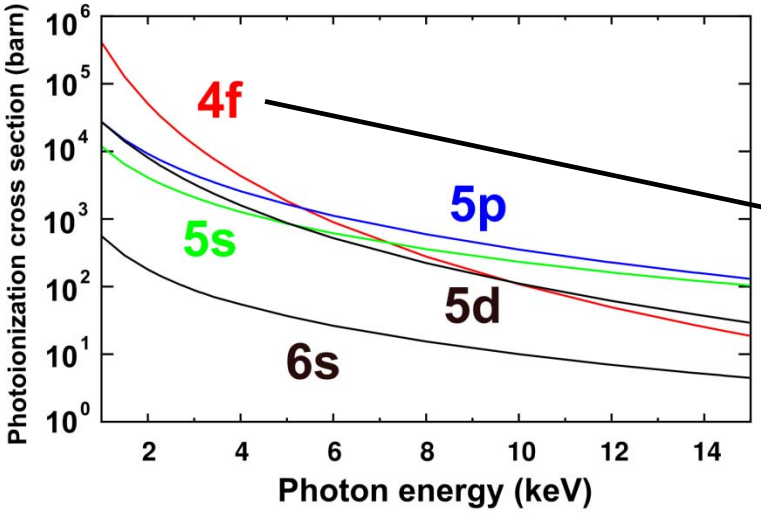

Experiment:

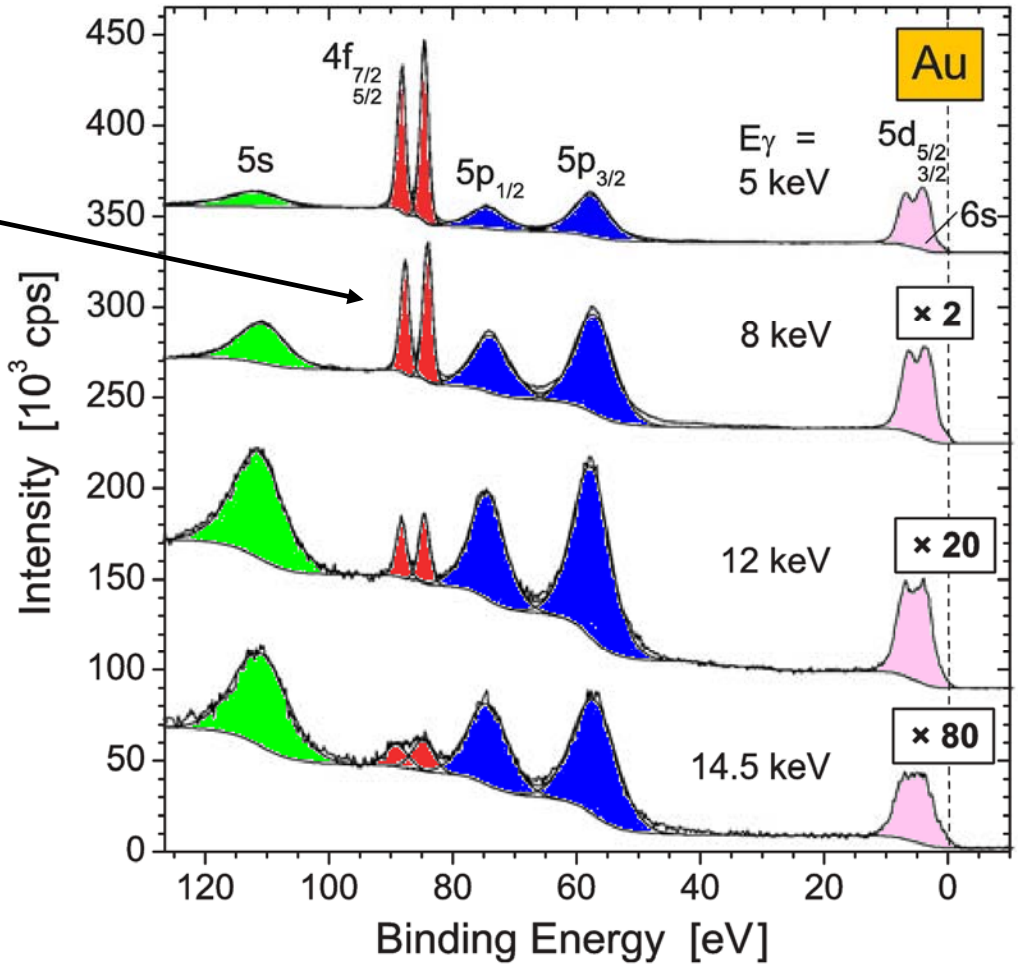

cross section for higher l decreases faster

energy dependence can be e.g. utilized to modulate partial density of states in VB

C. Kunz et al.
Nucl. Inst. Methods A 547, 73 (2005)

X-ray standing waves (Bragg)

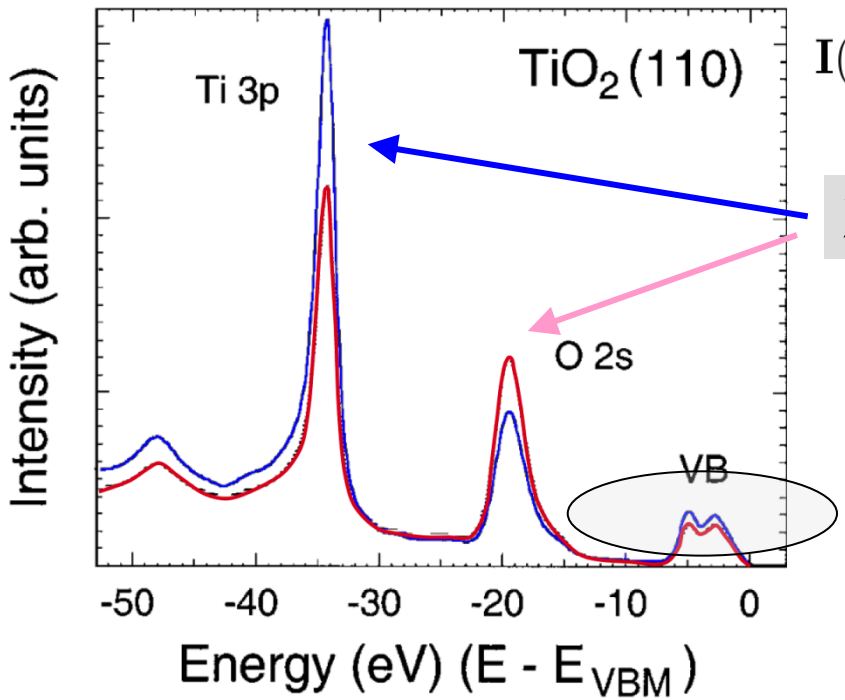

$$\mathbf{I(h\nu) \propto 1 + R(h\nu) + 2\sqrt{R(h\nu)}f_c\cos(\Phi(h\nu) - 2\pi P)}$$

XSW modulation

$$\mathbf{I(E, h\nu) \propto \sum_{i,l} \rho_{i,l}(E)\sigma_{i,l}(E, h\nu)}$$

weighting by PE cross section

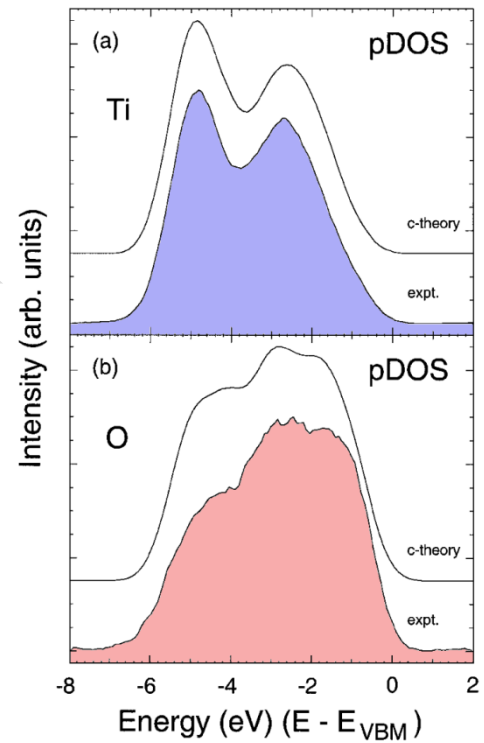

site specific VB decomposition into partial density of states

J.C. Woicik et al, PRL 89, 077401 (2002)

Angular dependence of photoelectric cross section

$$\frac{d\sigma_i}{d\Omega} = \frac{\sigma_i}{4\pi}[1 + \beta P_2(\cos\theta) + (\delta + \gamma\cos^2\theta)\sin\theta\cos\varphi]$$

dipole

quadrupole

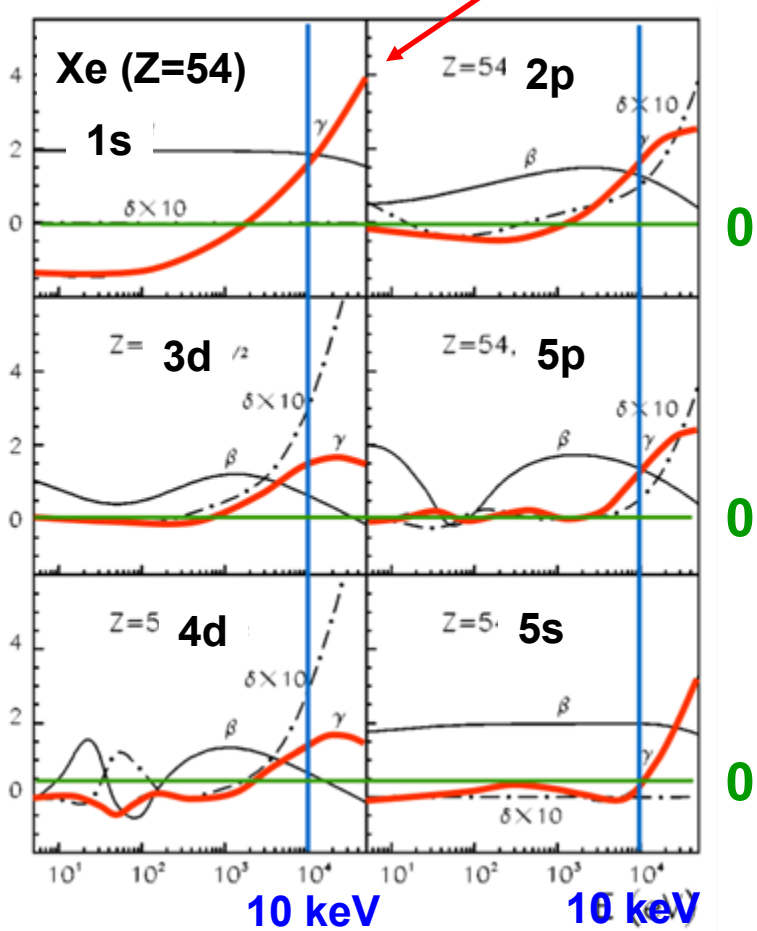

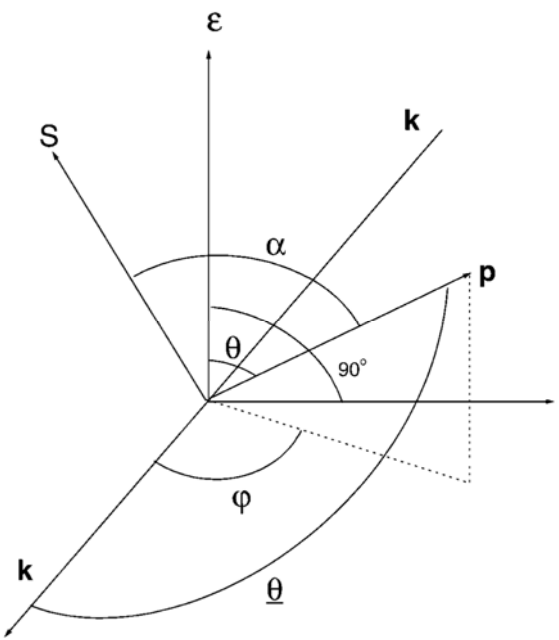

quadrupolar terms may not be neglected even at not so hard X-ray energies

TRZHASKOVSKAYA et al.
At. Data Nucl. Data Tables 77, 97 (2001)

what else ...

photoelectron recoil: not only core levels (light cores), but also VB

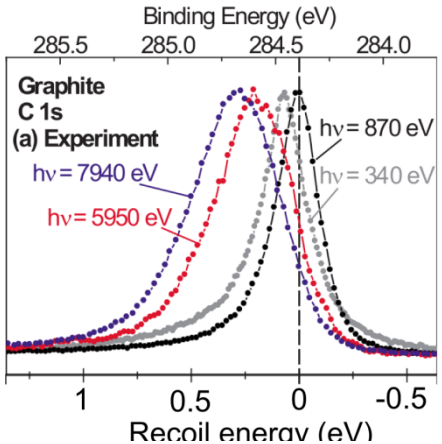

Y. Takata et al.
PRB 75, 233404 (2007)

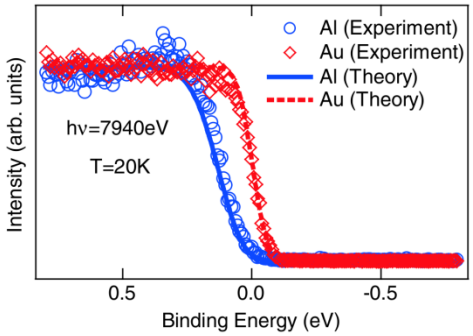

Y. Takata et al.
PRL 101, 137601 (2008)

also: photon momentum !
any chance for band structure studies?

In Hamburg back then ...

Bending magnet at DORIS II (~1989)
~5x10^9 ph/s into ΔE/E = 10^{-4}

counting rates:
~100 / sec

very tedious !

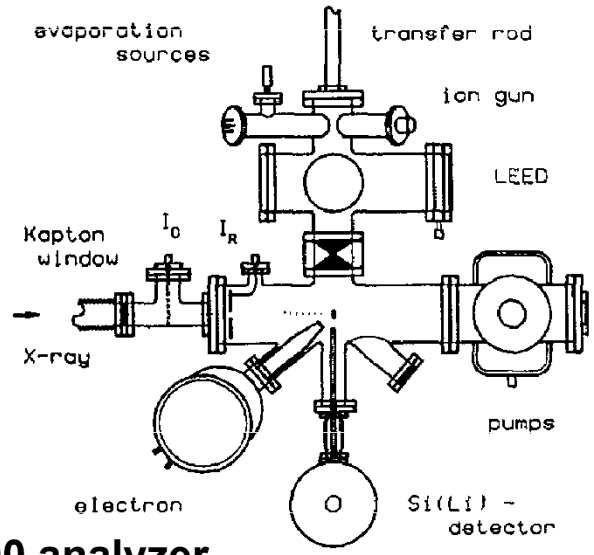

VG CLAM 100 analyzer
with „HV option“
single channeltron
E_{kin} up to ~5000eV

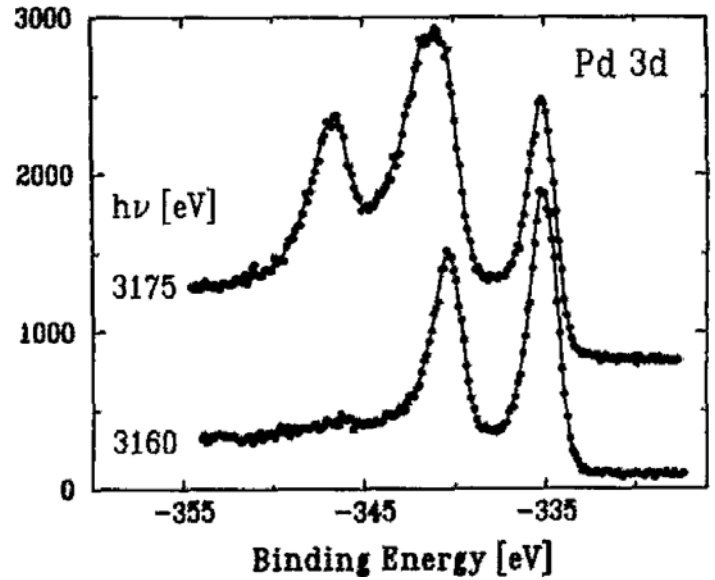

X-ray standing waves and X-ray photoemission measurements in the energy range 2.7-7 keV
W. Drube et al., Rev. Sci. Instrum. 83, 1138 (1992)

resonant Pd L_3-$M_{45}N_{45}$ excitation
ccc analog to the famous
Ni 6eV VB satellite

Photon sources at DESY

DORIS III

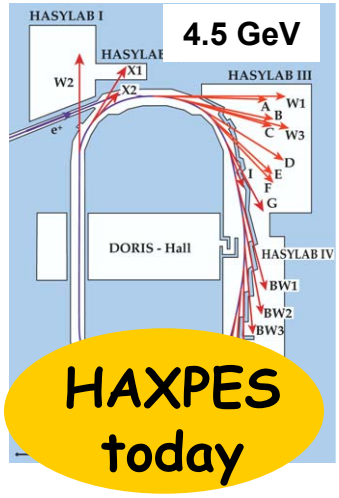

FLASH

PETRA III

XFEL

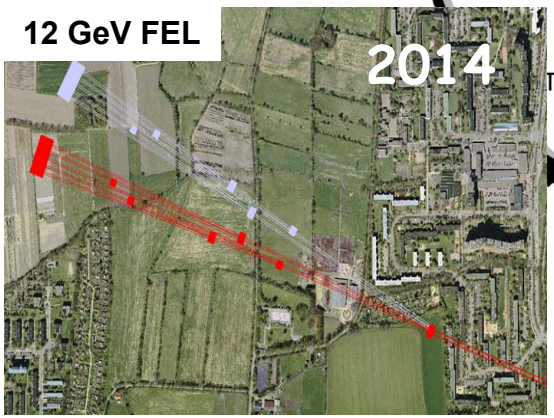

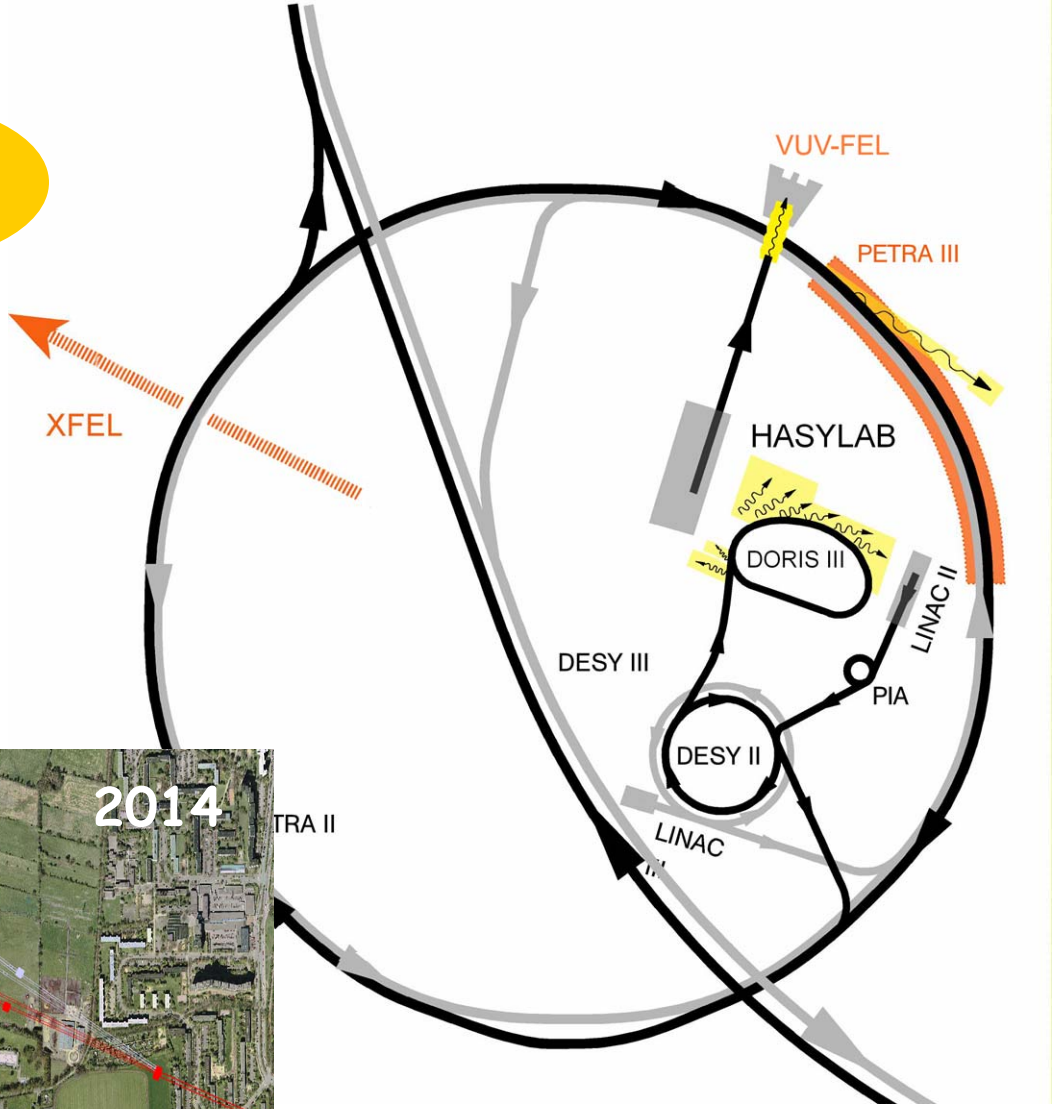

Currently: tunable HAXPES at DORIS III

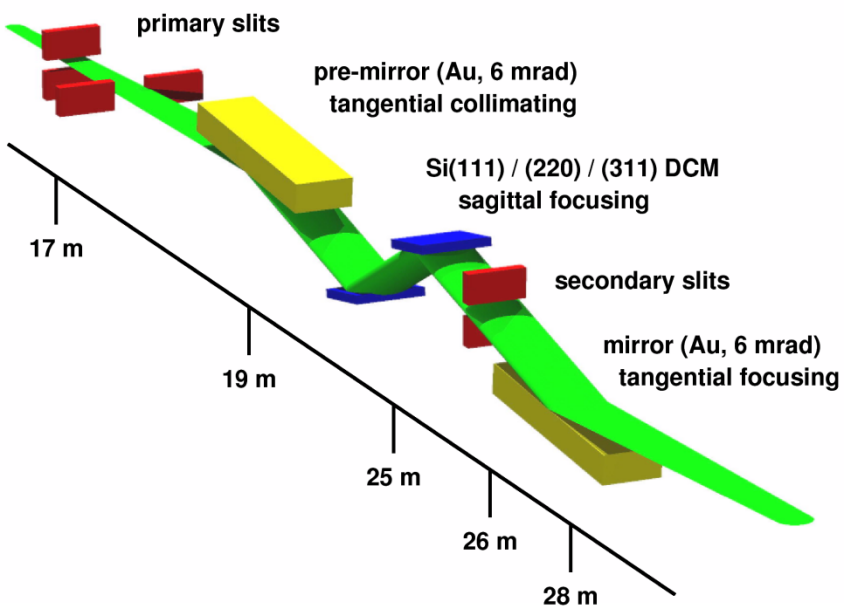

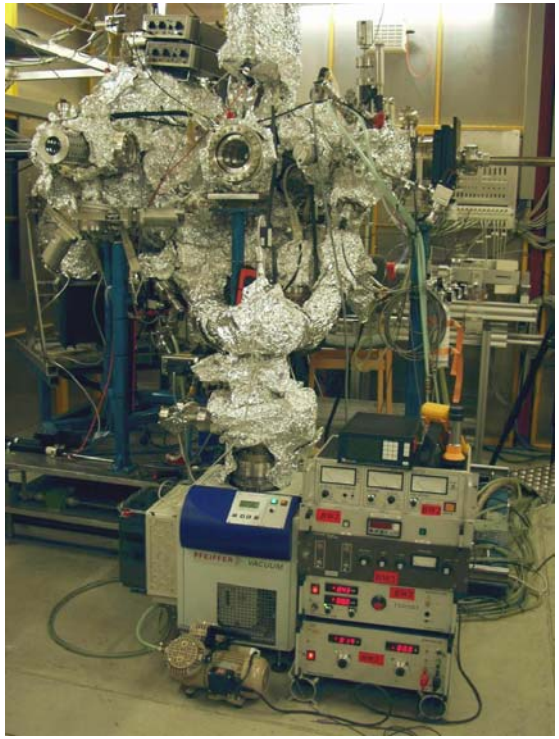

- X-ray wiggler beamline BW2
- Focal properties at the sample well adapted to the acceptance of the electron spectrometer ("no photons lost")
- Dedicated stationary XPS instrument
- Experiments started in 1995 with Scienta SES-200 analyzer
- Energy range: photons 2.2-10 keV,
  electrons up to 5 keV (7.5 keV with sample bias)

DORIS III HAXPES instrument

focus
0.15 x 2 mm^2

Si(111) flux
5 x 10^{12} s^{-1}

very well matched to analyzer acceptance!

Analyzer („ancient“ Scienta SES-200)

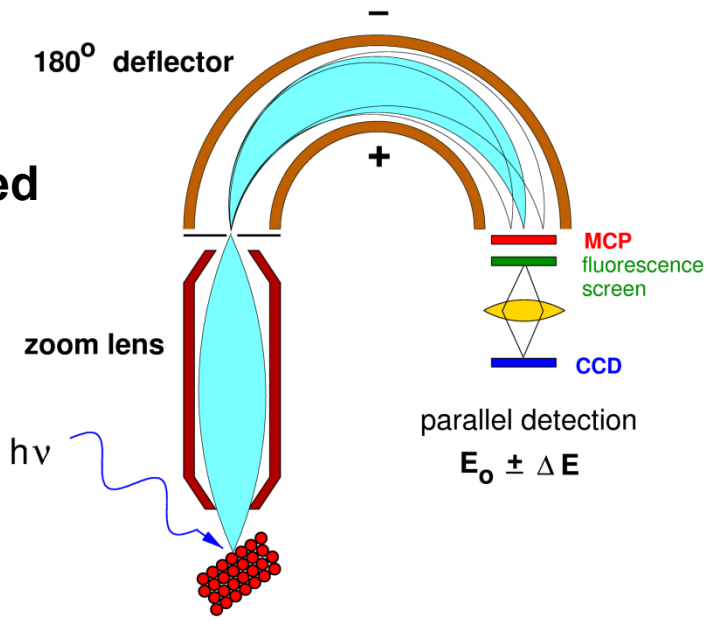

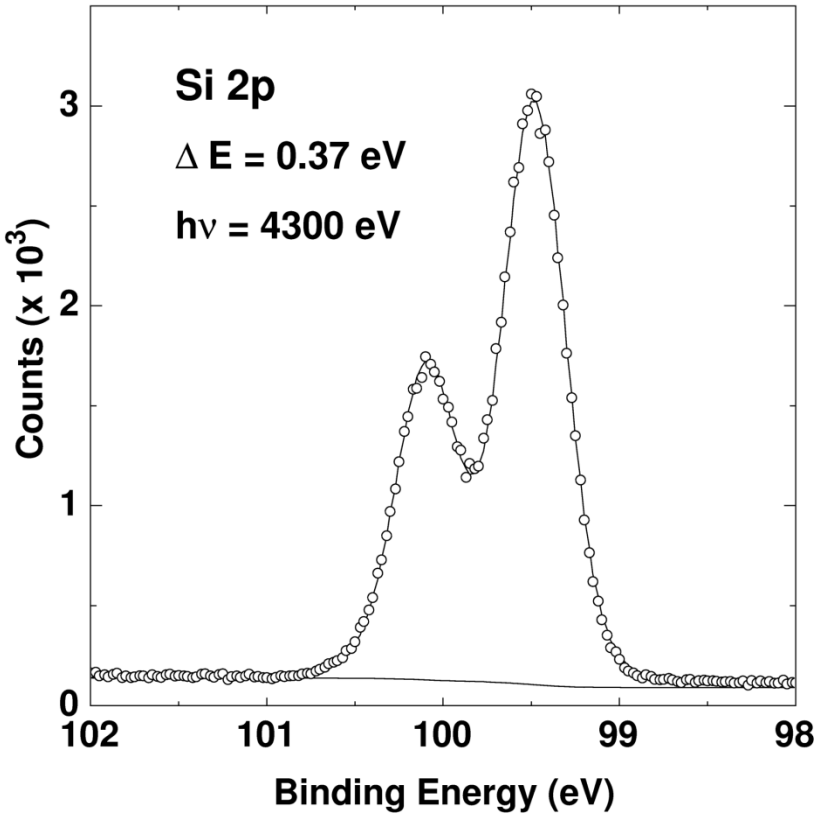

Energy resolution is source limited, but sufficient for most core-level studies

benchmark:
Si 2p using Si(311) monochromator

Si 2p intrinsic line width: 0.07 eV
J. Woicik et al., PRB 40, 12463 (1989)

Buried layers

PbS/EuS/PbS multilayers

(spintronics)

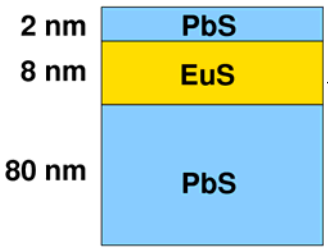

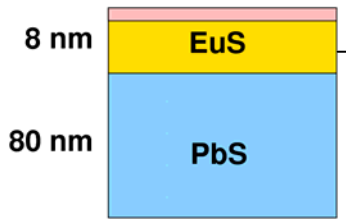

hν = 3510 eV

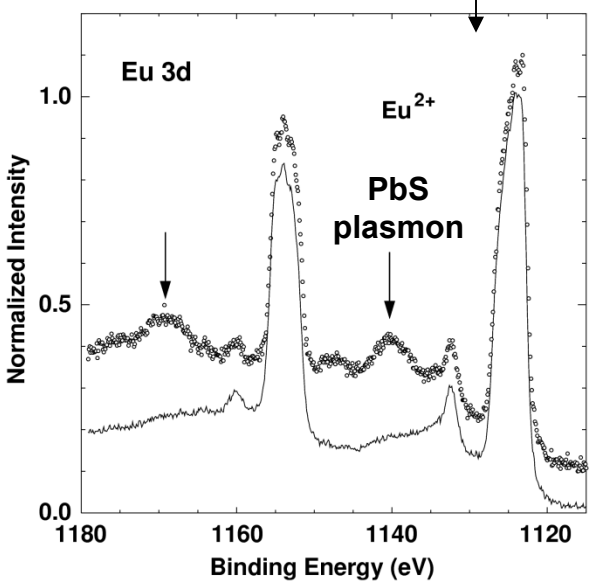

Eu 2+ in the buried layer

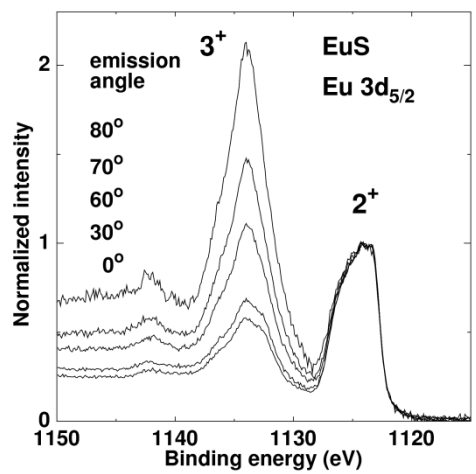

Eu 3+ near "open" surface

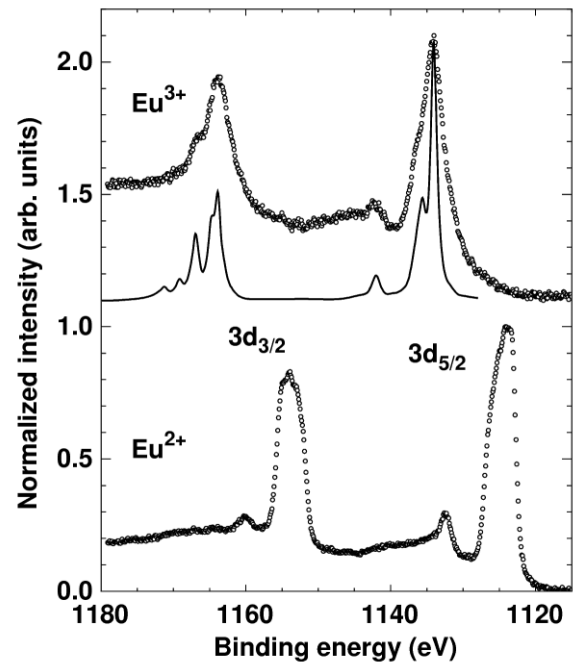

combine spectra linearly to discriminate surface and bulk

B.A. Orlowski et al.
J. El. Spec. Rel. Phemon. 137-140, 763 (2004)

Buried layers

PbS/EuS/PbS multilayers

Note: no matter how large the escape depth, the top layers are always present

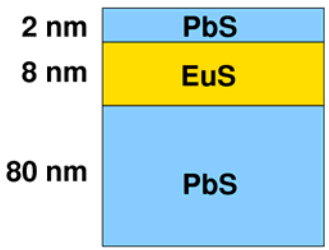

$h\nu$ = 3510 eV

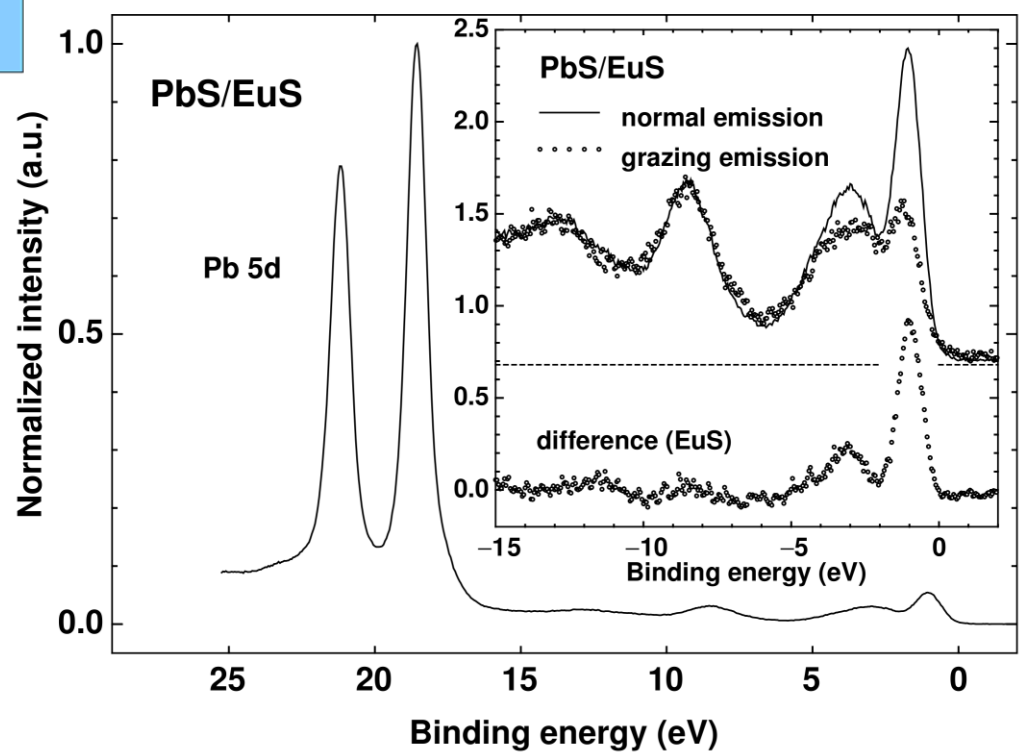

Eu & Pb overlapping in the valence band

Also: good understanding and modelling of inelastic loss processes needed

B.A. Orlowski et al.
J. El. Spec. Rel. Phemon. 137-140, 763 (2004)

MnO: Mn 2p fine structure

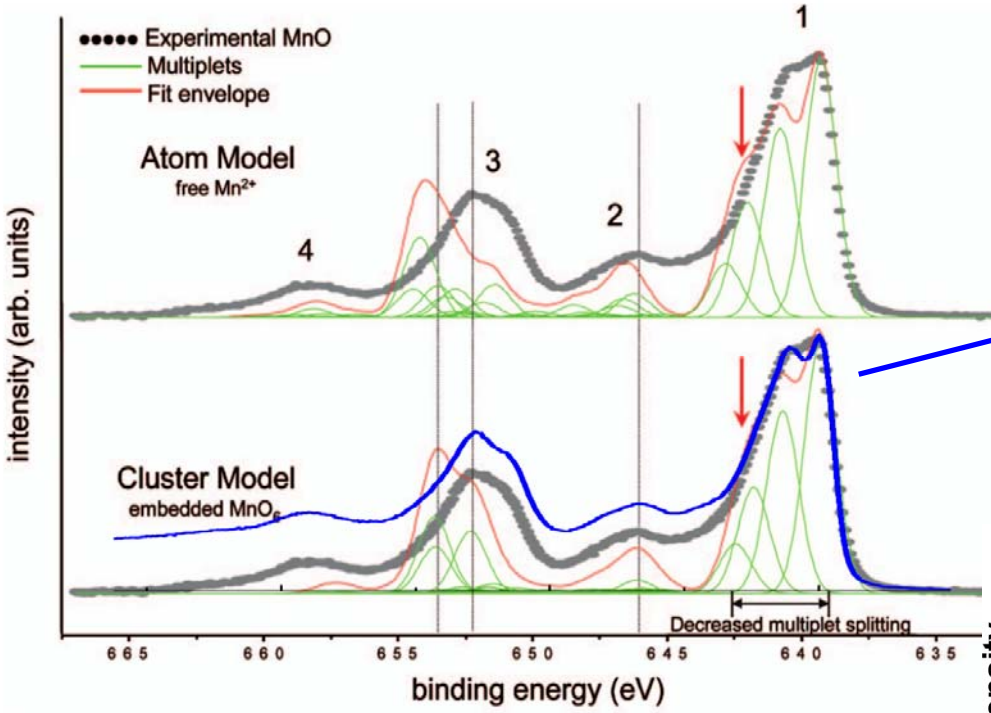

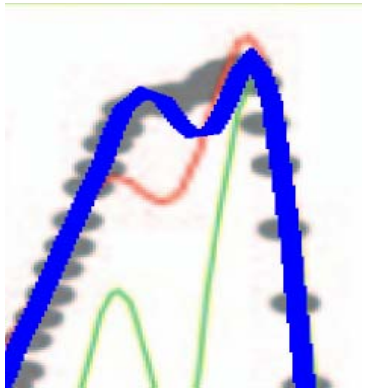

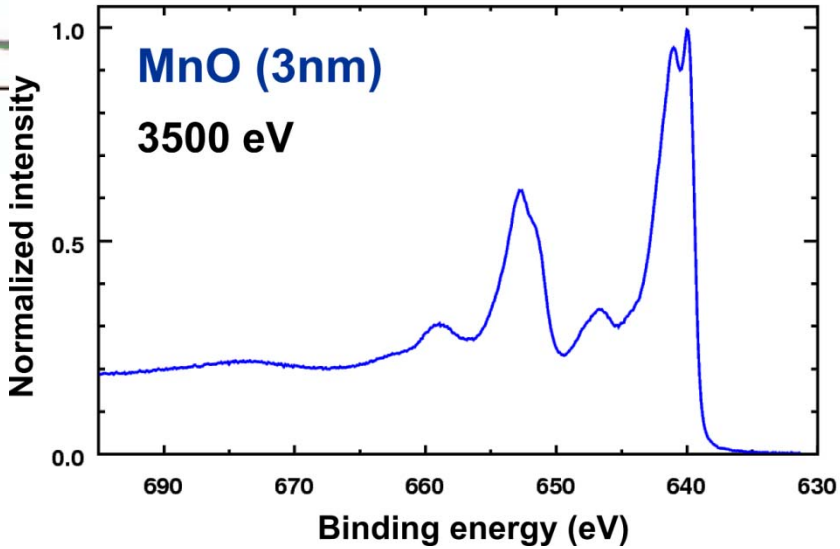

Theory: Bagus et al, PRB 73, 155110 (2006)

MnO_6 cluster model (including covalency, but no CT):
peaks and shapes well reproduced
smaller splitting than atomic Mn^{2+}, better agreement with experiment (but still too large)

except peak 4: extrinsic plasmon?
HAXPES (thin film) -> no -> intrinsic feature
possibly CT configurations (not yet included)

MnO: valence band structure

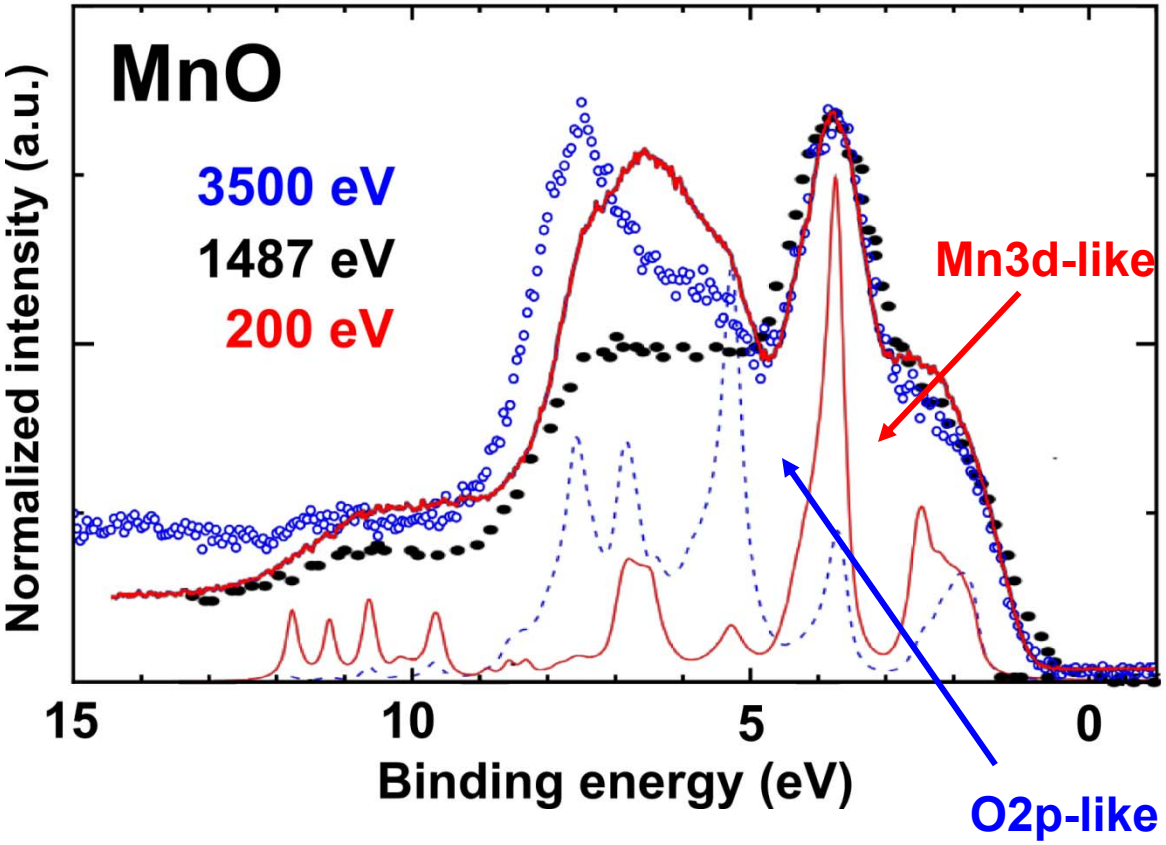

Experiments:

van Elp et al, PRB 44, 1530 (1991)
MnO bulk

M. Nagel et al, PRB 75, 195426 (2007)
4nm on Ag(001), difference spectrum

BW2 data (3nm on carbon)

Theory:
R. Eder, PRB 78, 115111 (2008)
(variational cluster approximation)

„Bulk“ materials characterization

Surface segregation of interstitial manganese in $Ga_{1-x}Mn_xAs$

x ~ 0.05

ferromagnetism combined with semiconductor technology (x ~ 1% - 8%)

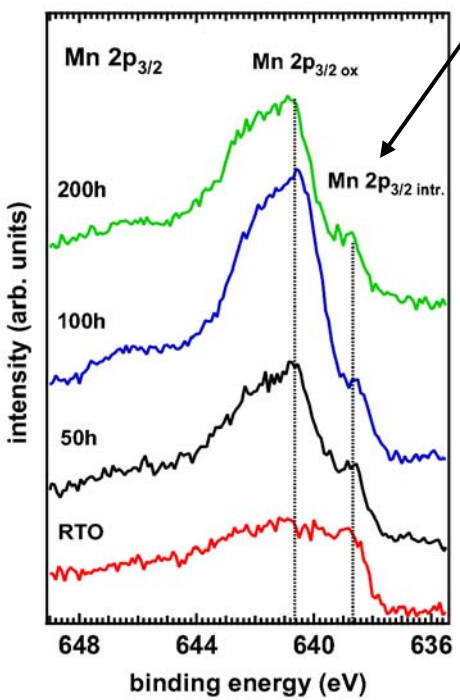

annealing

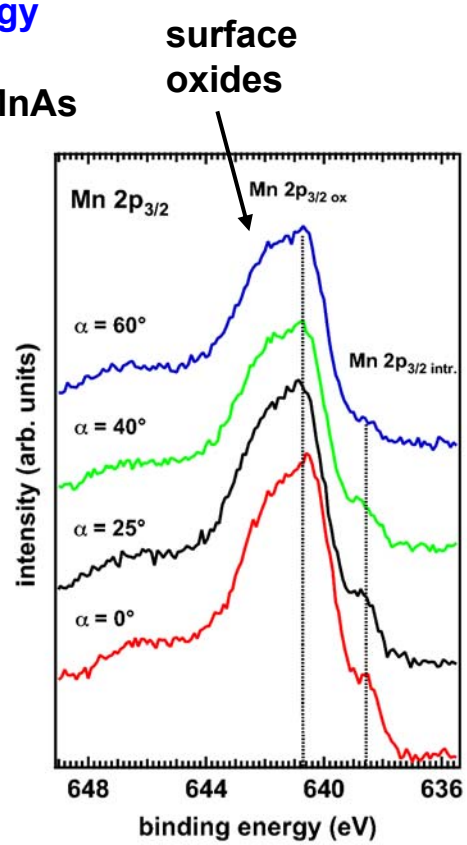

„depth profiling“

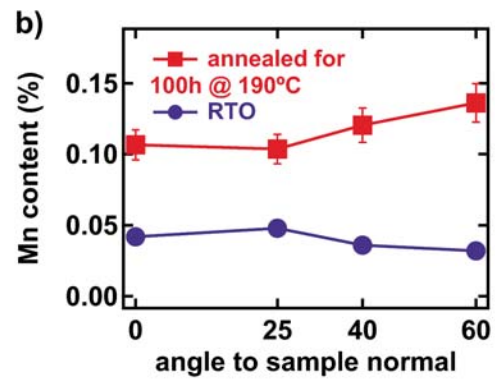

surface segregation

homogeneous

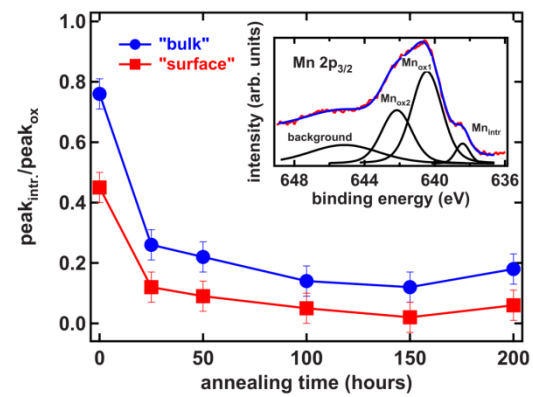

B. Schmid et al., PRB *78*, 075319 (2008)

Resonant inner-shell transitions

Threshold excitation of inner-shell Auger cascades

- Dynamics of core hole formation
- Interplay between solid state (band) and atomic behavior
- d-metals: localized and de-localized valence levels
- Band filling: closed shell vs. open shell
- Localized intermediate excited states (e.g. "white lines")
- Auger satellites (electron correlation)
- Examples: 3d metal $K\text{-}L_{2,3}L_{2,3}$ (inner shells only)

Resonant inner-shell transitions

3d metal KLL Auger satellite structure

Non-resonant Cu K-$L_{2,3}L_{2,3}$

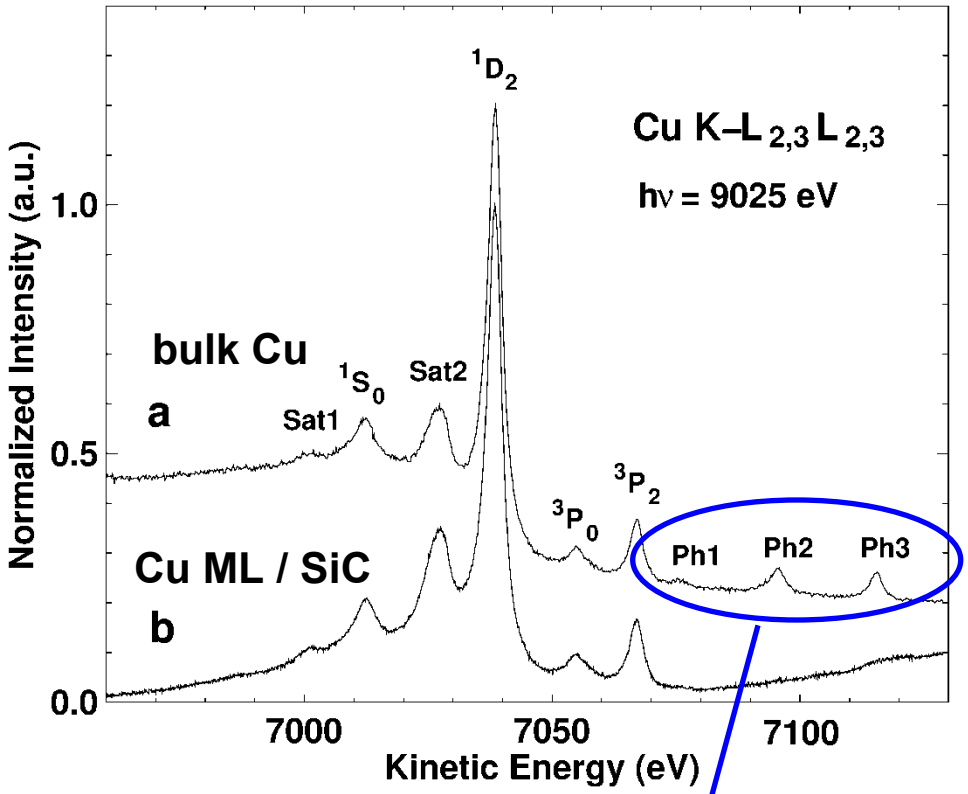

internal photoemission: Kα excited 2p shell

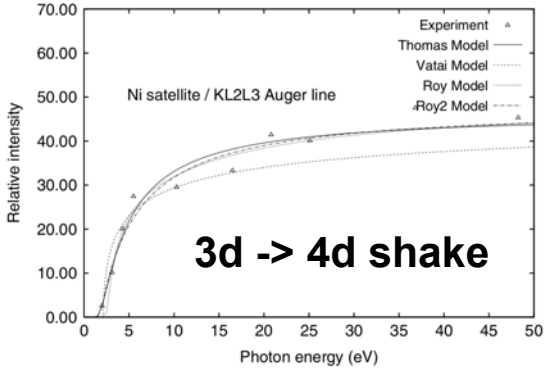

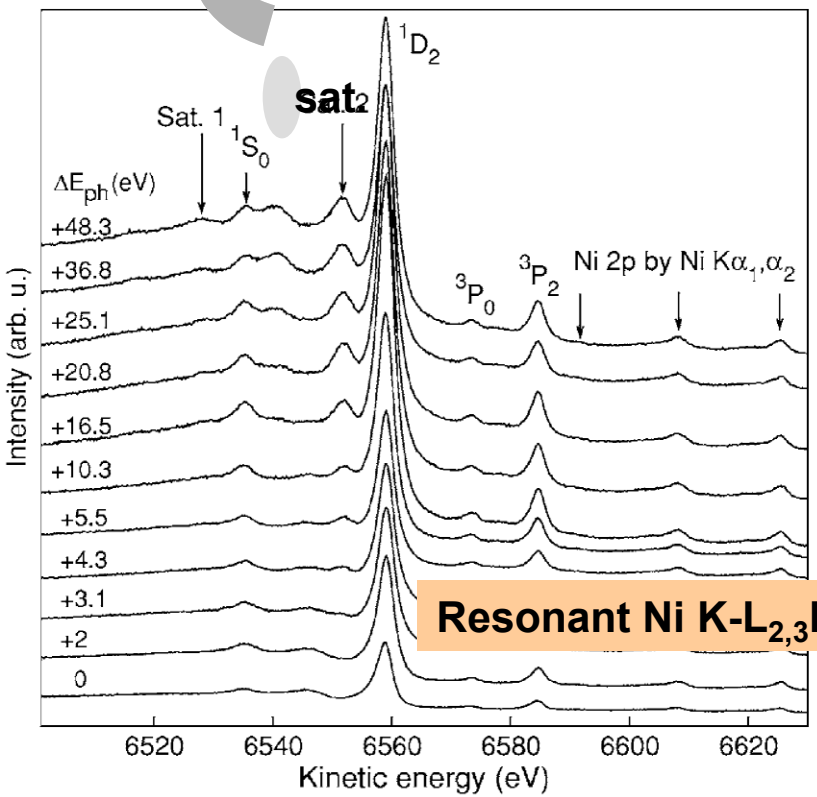

Resonant Ni K-$L_{2,3}L_{2,3}$

L. Köver et al, PRB 73, 195101 (2006)

Resonant inner-shell transitions

Resonant Ti $KL_{2,3}L_{2,3}$ from rutile $TiO_2(110)$

Energetically separate resonating Auger transitions → Identification of dipole and individual quadrupole components (t_{2g}, e_g) in the pre-K-edge structure $TiO_2(110)$

J. Danger *et al.*, PRL 88, 243001 (2002).

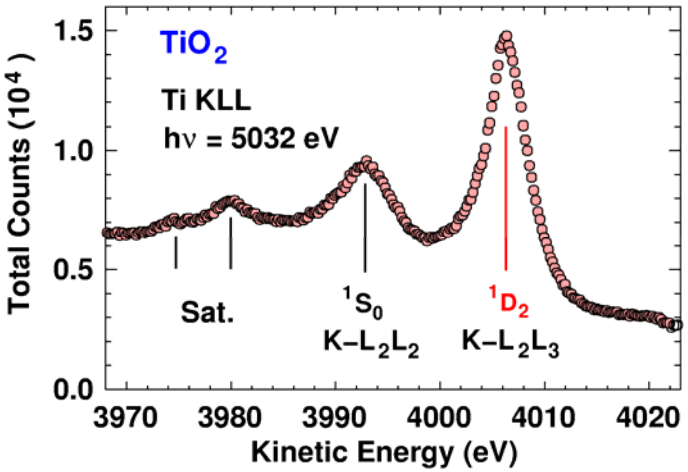

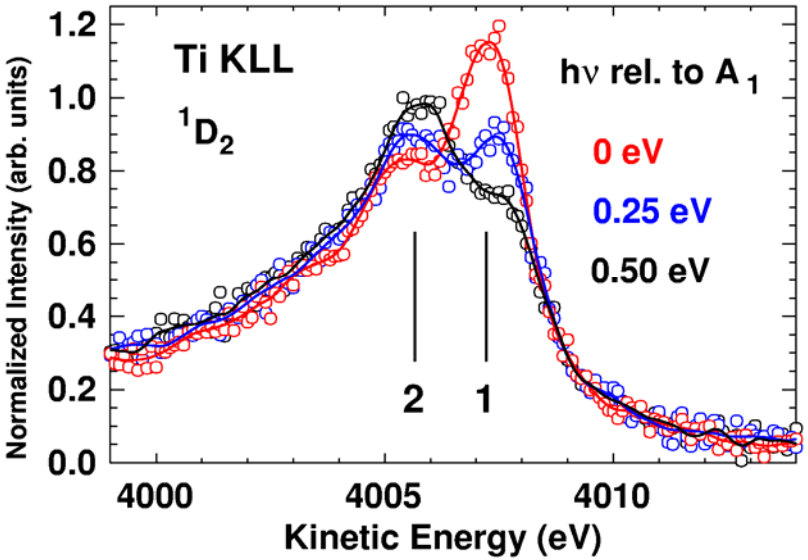

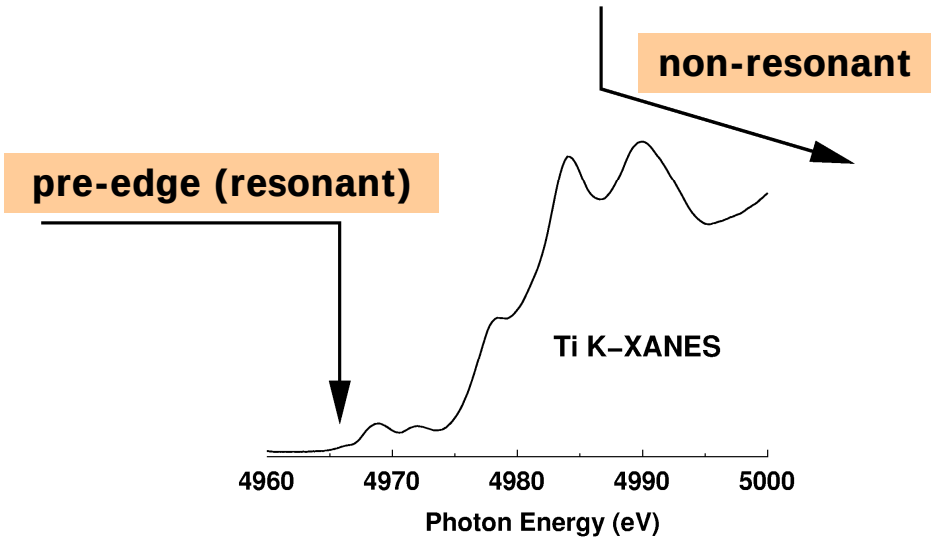

Resonant inner-shell transitions

Resonant Ti KLL from rutile TiO_2(110)

(HAXPES instrument @ BW2, HASYLAB)

Ti K pre-edge:
Ti $KL_{2,3}L_{2,3}$ (^1D) Auger line splitting

→ different final states
→ detailed dipole / quadrupole contributions in pre-peak region (not obtained from XAS)

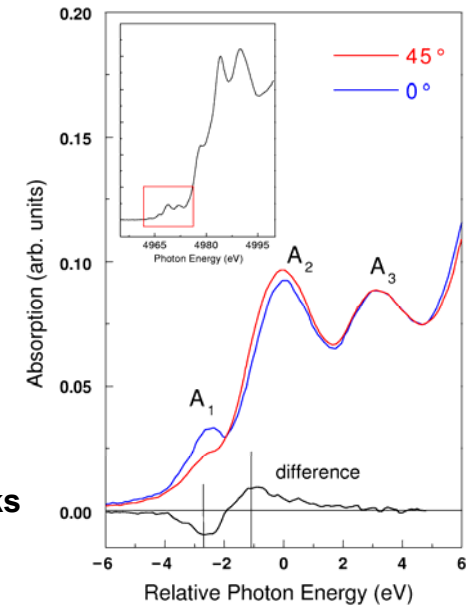

TiO_2(110)
K-edge pre-peaks

D dipole transition
Q_1 $1s \rightarrow d_{xz}, d_{yz}$ (t_{2g})
Q_2 $1s \rightarrow d_{x^2-y^2}, d_{z^2}$ (e_g)

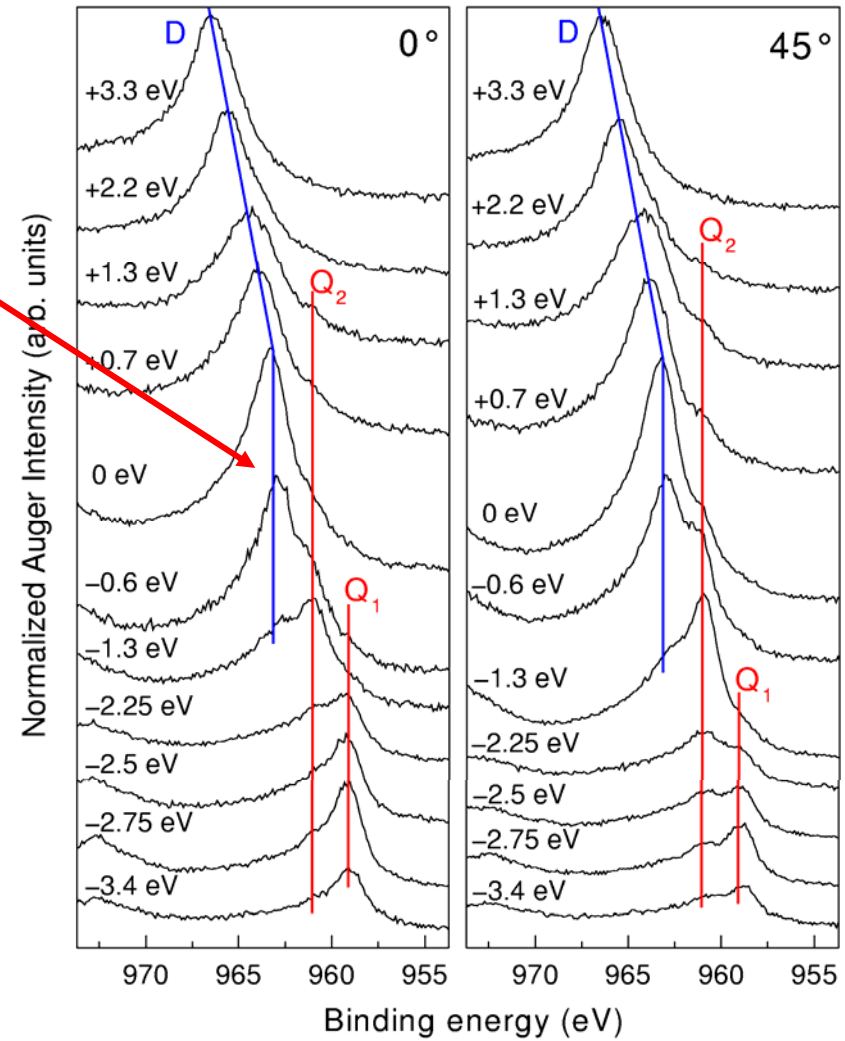

J. Danger et al., PRL 88, 243001 (2002)

Final state relaxation

SiO_2 /Si interface: Si 2p "chemical shift"

(known for over 25 years, no clear conclusion yet)

Relative Si 2p BE (SiO_2 vs. Si(100) bulk)

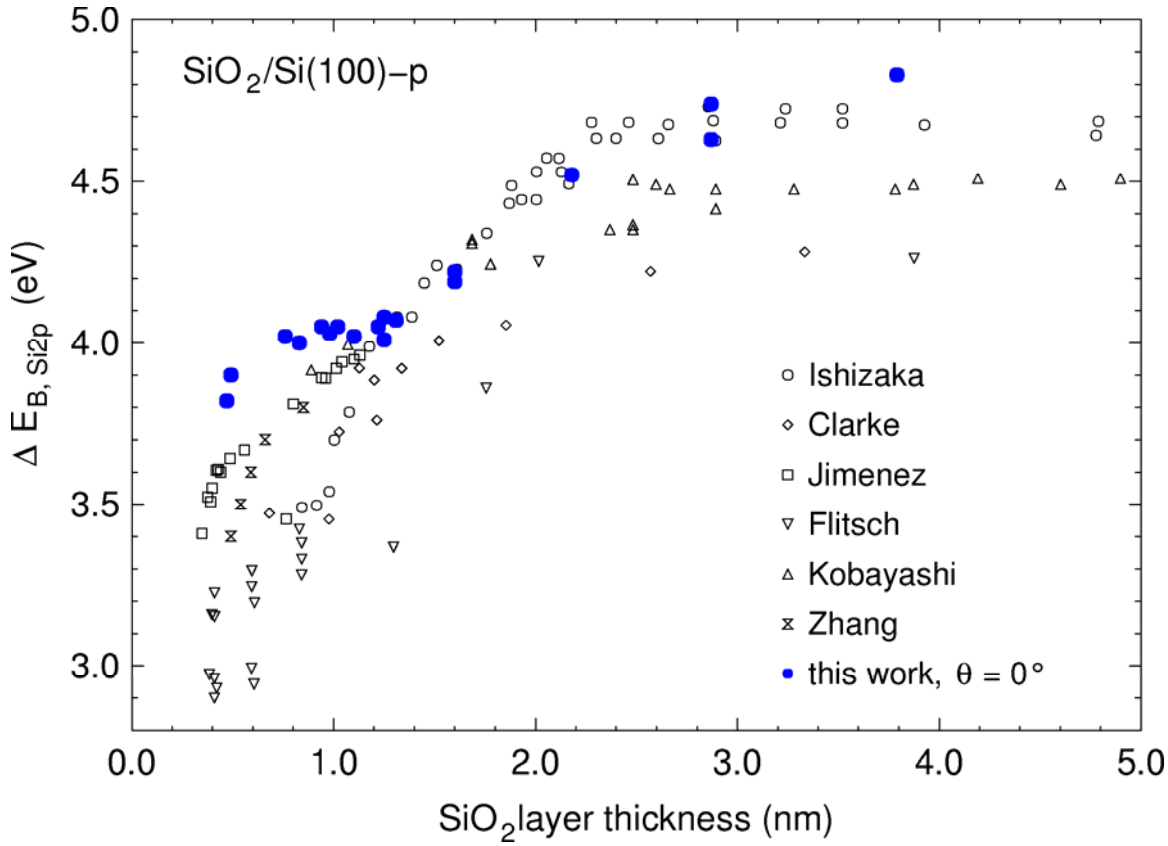

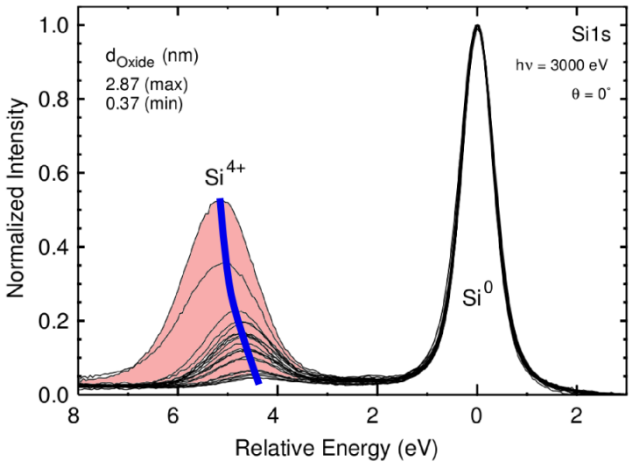

models discussed:

- **extended strain fields**
- **bond strain**
- **second nearest-O effect**
- **charge trapping**
- **local electronic relaxation**
- **image potential (non-local)**

Final state relaxation

Generalized Auger parameter: separate ΔE_i and ΔR

$$\Delta E_B = \Delta E_i + \Delta R$$

Here: purely inner-shell transition (CCC)
Consider only differences:
then $\Delta R = \Delta R_{extra-atomic}$

Measure 1s, 2p, KLL energy differences:
then $\Delta R_{ea}^{2p} = \frac{1}{2}\Delta\xi(1s, 2p, 2p)$

where:

$$\Delta\xi(1s, 2p, 2p) = \Delta E_{kin}^{KLL} - \Delta E_B^{1s} + 2\Delta E_B^{2p}$$

Likewise:

$$\Delta E_i^{2p} = \Delta E_B^{2p} - \frac{1}{2}\Delta\xi(1s, 2p, 2p)$$

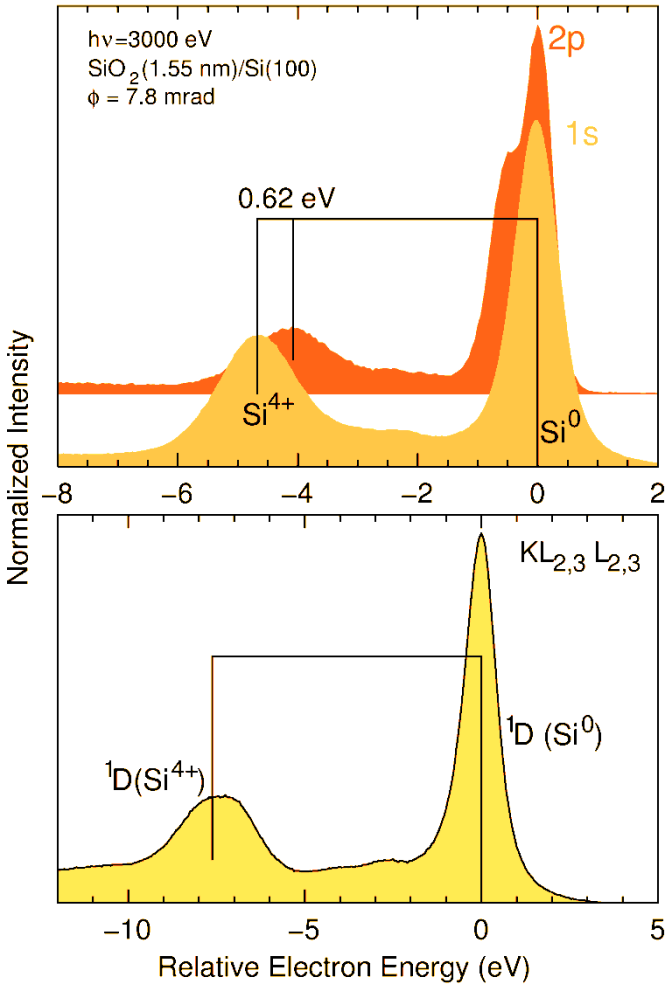

G. Hohlneicher et al, J. El. Spec. Rel. Phenom. 37, 209 (1985)

Dependence on oxide thickness

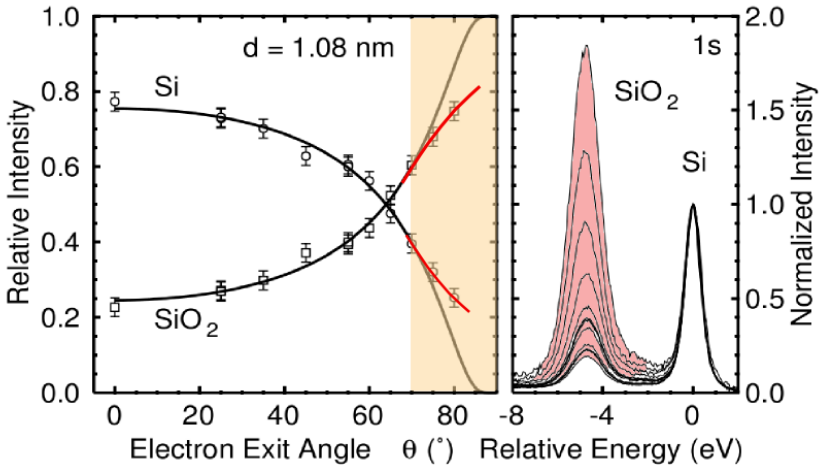

ΔE for Si 1s, 2p and $KL_{2,3}L_{2,3}$

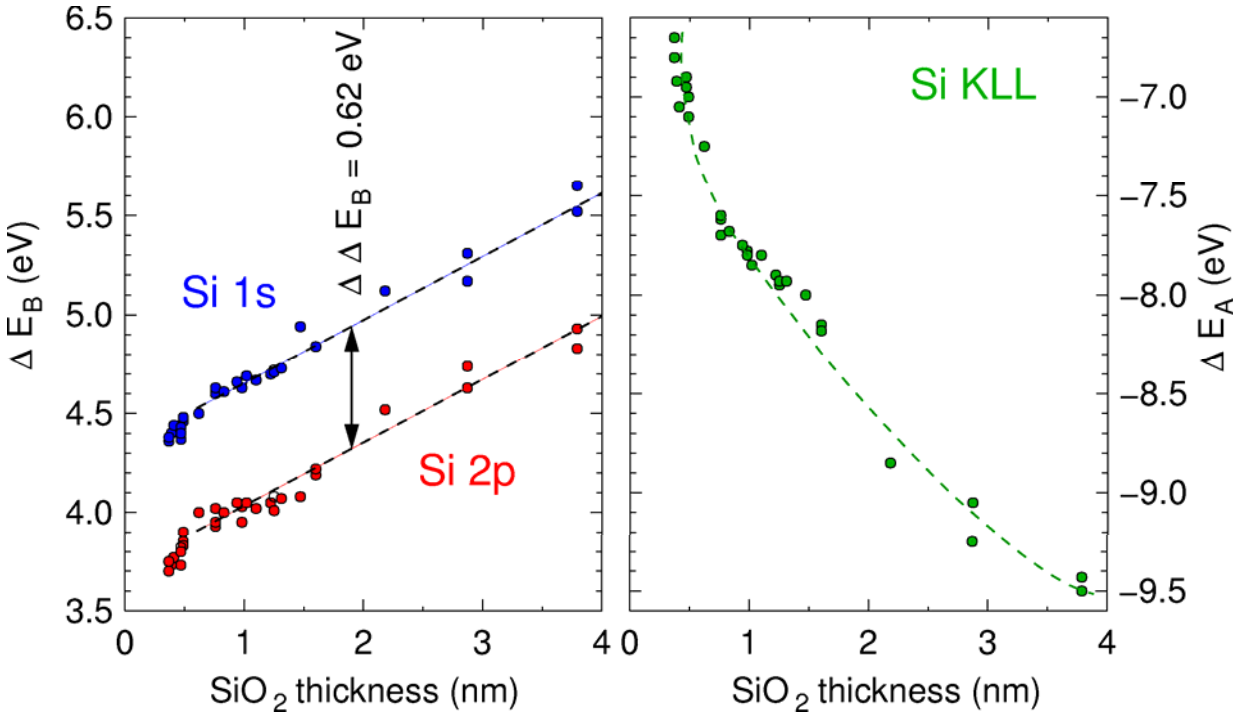

ΔE (1s) – ΔE (2p)
= const (0.62 eV)

related to charge state

experiment: independent of oxide thickness

Th. Eickhoff et al, J. El. Spec. Rel. Phenom. 137-140, 85 (2004)

Final state relaxation

Contribution of image potential?

qualitatively: yes
quantitatively: no

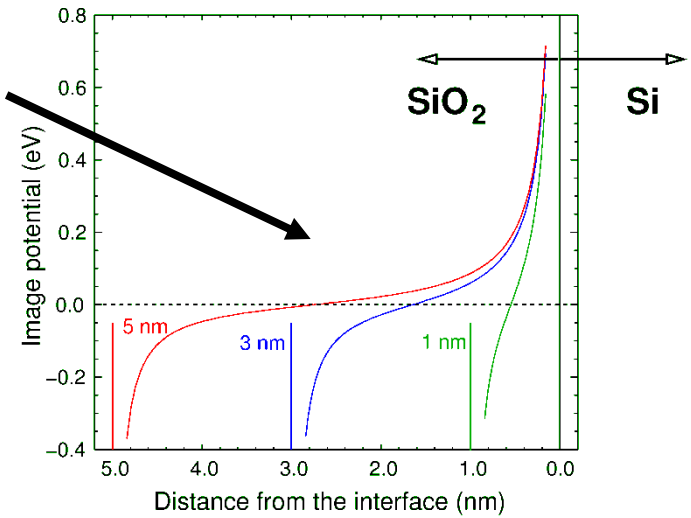

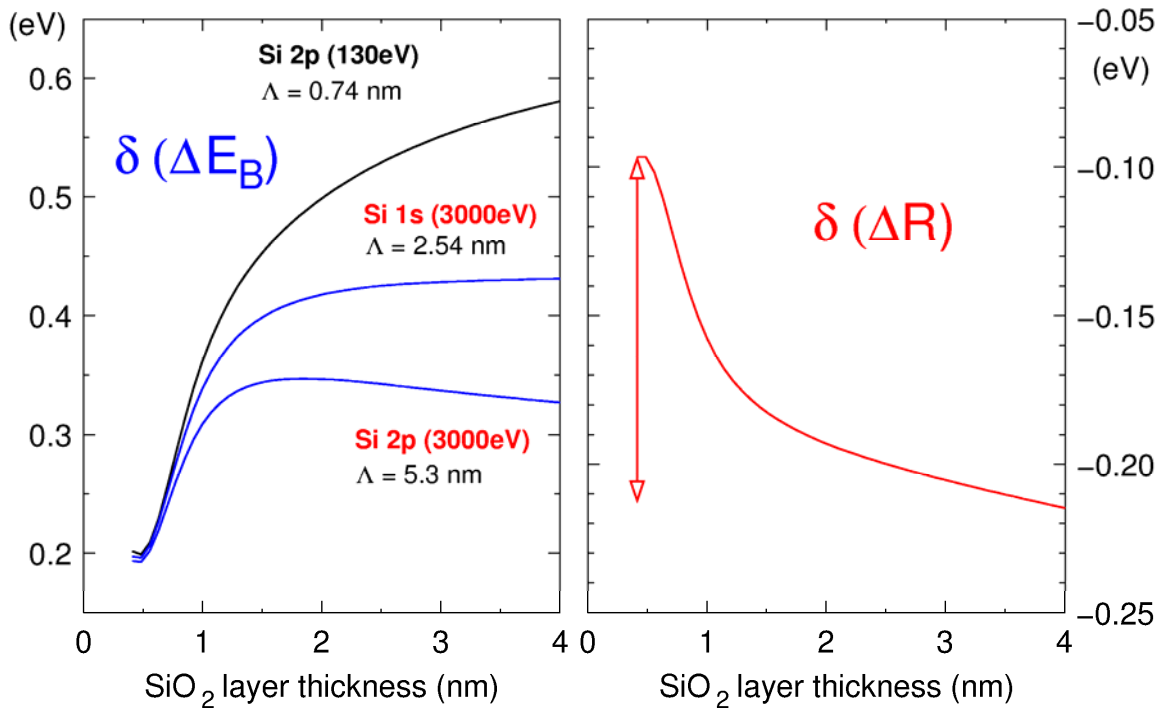

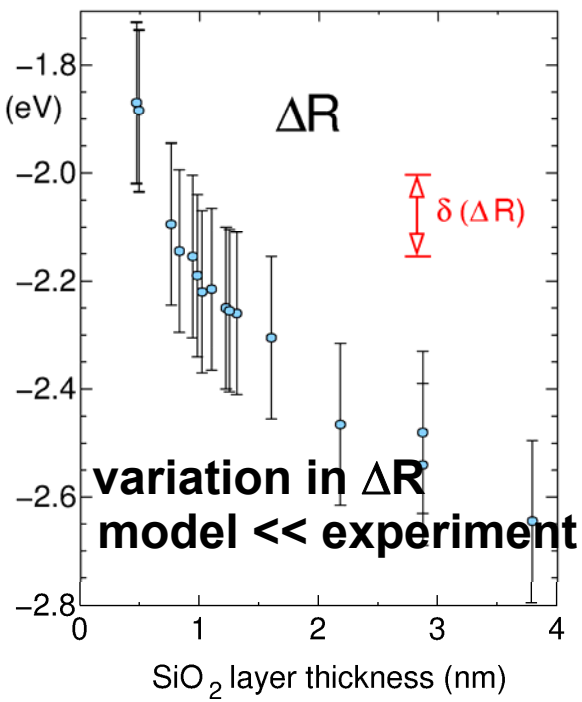

Initial state

Si 2p initial state differences

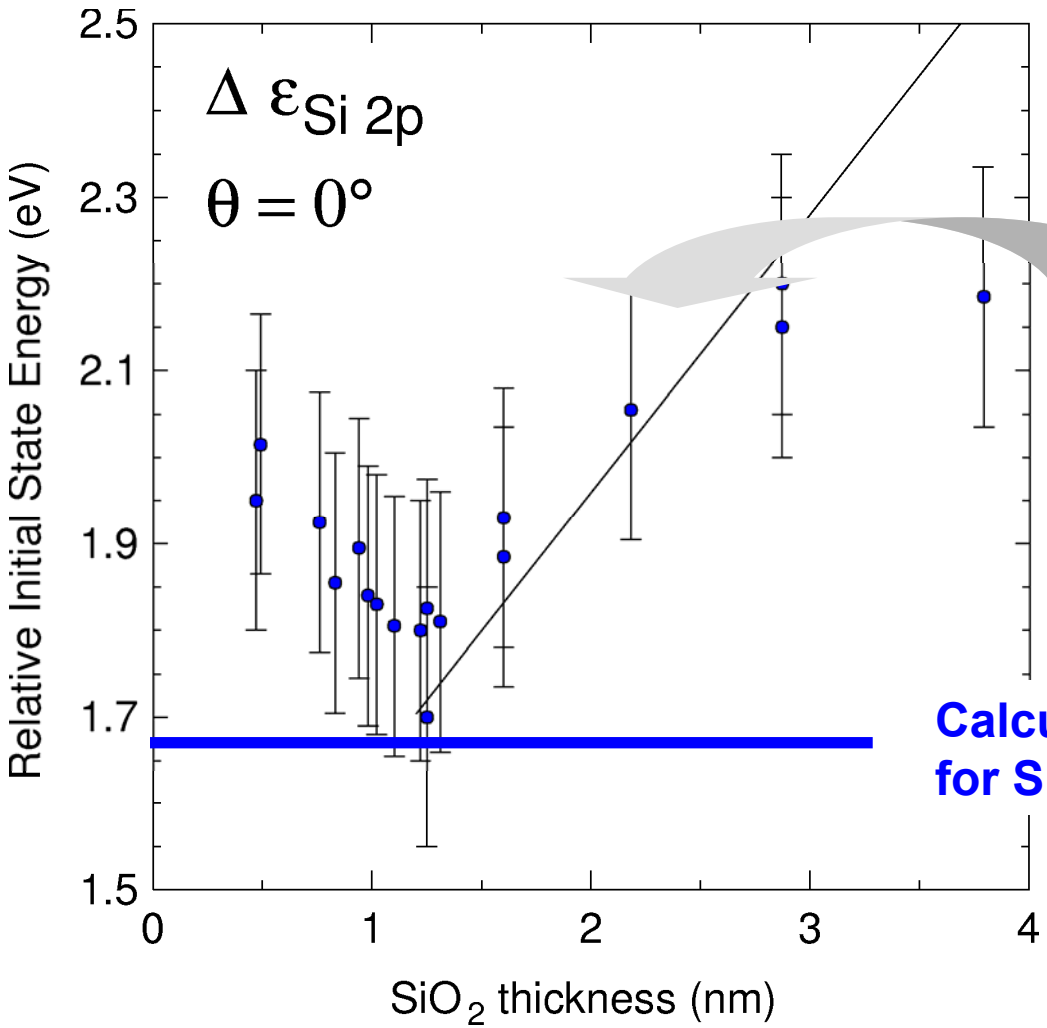

charge trapping starts here

Calculated (LDA) initial state shift for $SiO_2(SiH_3)_4$ "test molecules"

A. Pasquarello et al, PRB 53, 10942 (1996)

New source: PETRA III

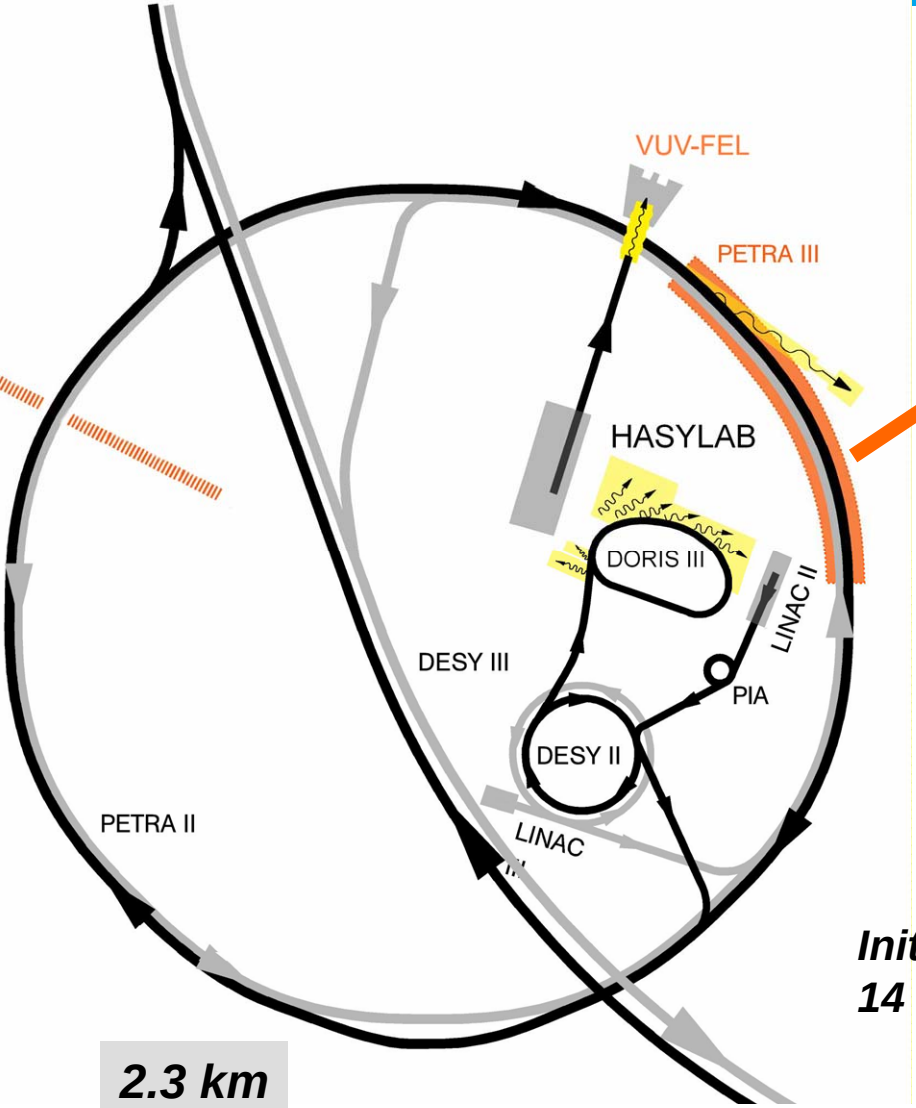

2.3 km

6 GeV / 100 mA (200 mA)
1 nmrad emittance
top-up mode operation

Designed to become the most brilliant hard X-ray storage ring source

Initial phase:
14 undulator beamlines, ~ 20 end stations

including a HAXPES instrument !

PETRA III source characteristics

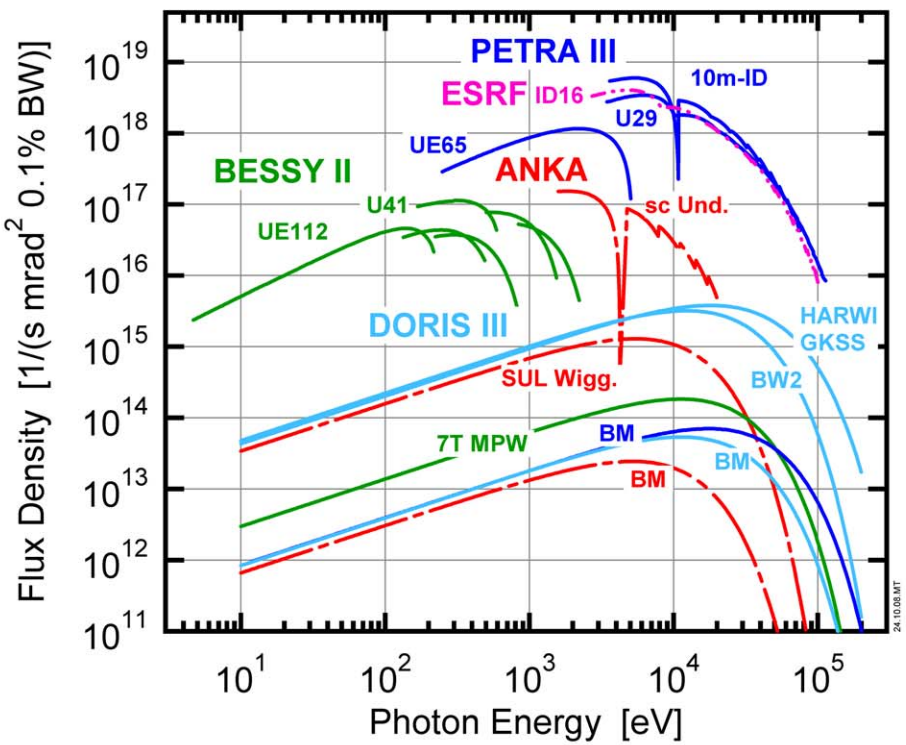

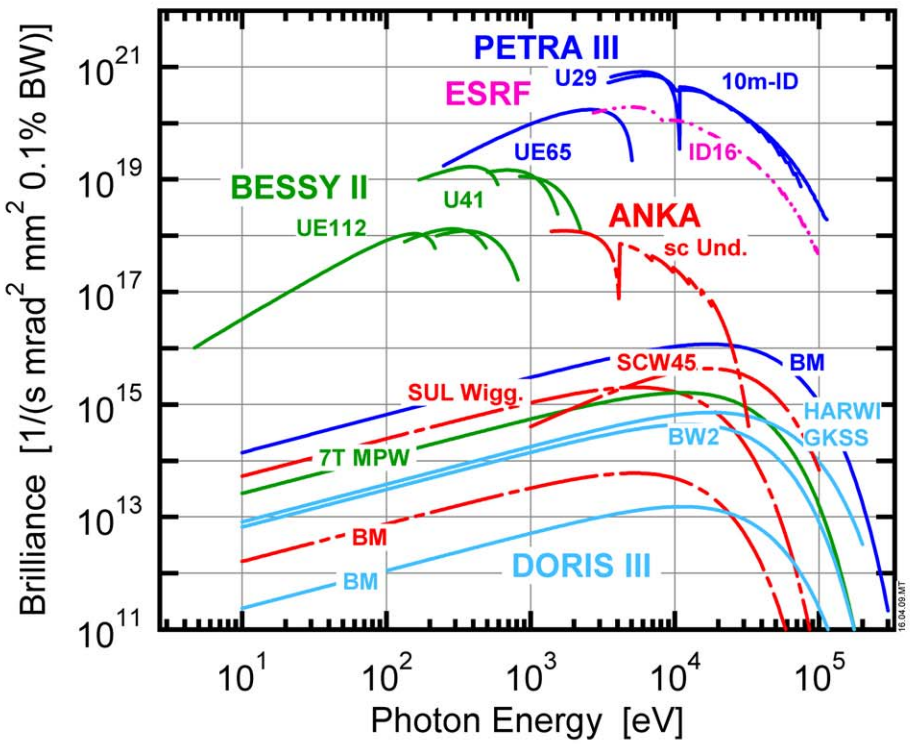

Photon beam parameters at 12keV:

	β_x [m]	β_y [m]	σ_x [μm]	σ_y [μm]	$\sigma_{x'}$ [μrad]	$\sigma_{y'}$ [μrad]	ID-length [m]
low-β 5 m	1.3	3	35.9	5.7	28	5.0	5
high-β 5 m	20	2.38	141	5.2	8.6	5.2	5

coherent flux:
- **12keV ($B(\lambda/2)^2$)**
- **1×10^{11} ph/s/0.01%BW**

Horizontal β-function of each straight section can be selected individually and is changeable (β_x= 1.3m or β_x = 20m)

PETRA III undulator beamlines

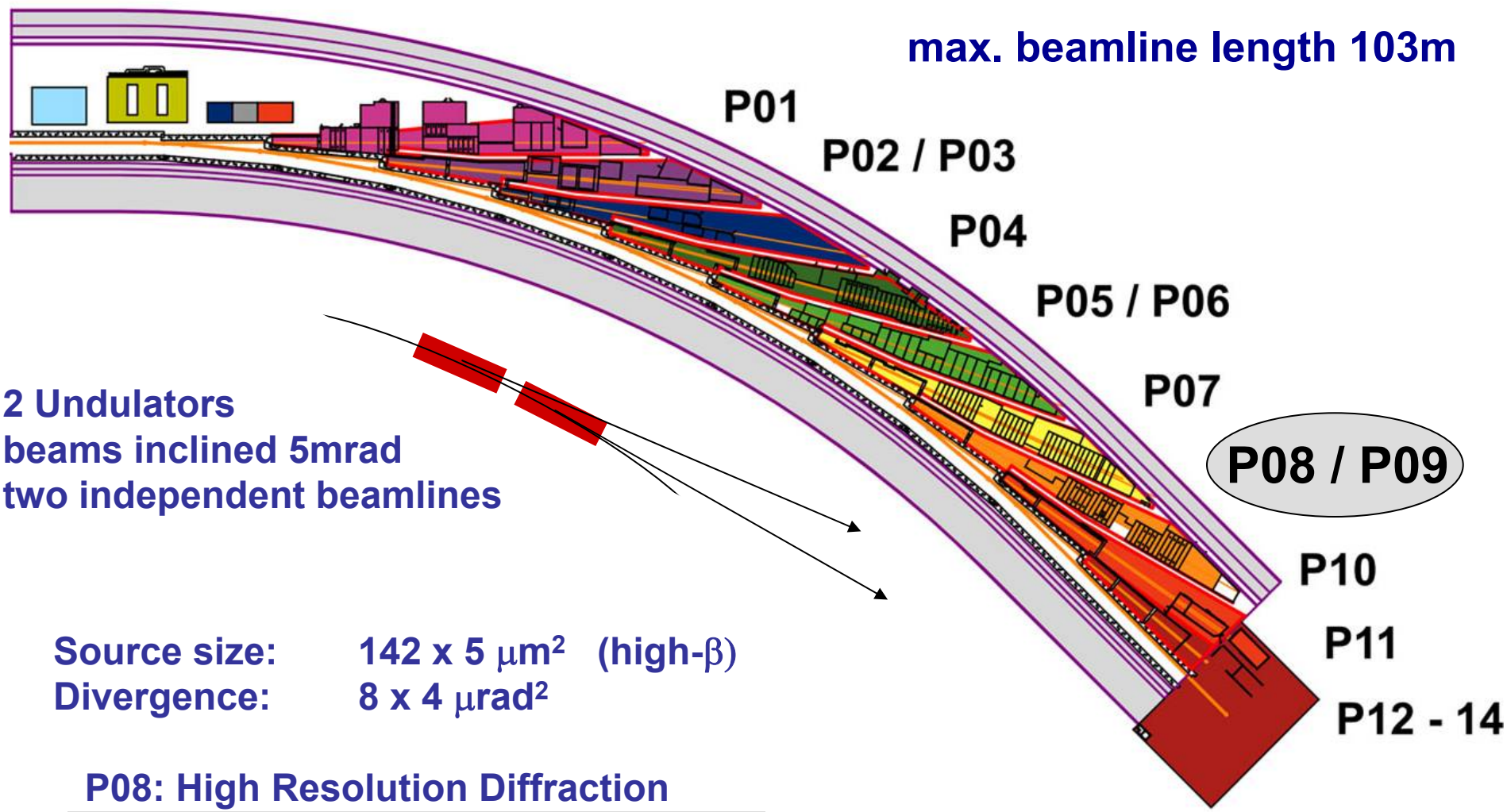

2 Undulators
beams inclined 5mrad
two independent beamlines

Source size: 142 x 5 μm^2 (high-β)
Divergence: 8 x 4 μrad^2

P08: High Resolution Diffraction

P09: Resonant Scattering & HAXPES

PETRA III undulator beamlines

applications which use the high source brilliance and capabilities for µ- and nano-focusing

BL	Name	ID-Typ	Energy range	Comment	Contact
P01	NRS, ps-time resolved, IXS	10 m U	6 - 40 keV		H. Franz, DESY
P02	Hard X-ray scattering/diffraction	2 m U23	8 - 100 keV	straight	H.-P. Liermann, DESY
P03	Micro SAXS/WAXS	2 m U29	8 - 23 keV	down	S. Roth, DESY
P04	Variable Polarization XUV	5 m UE65	0.2 - 3.0 keV		J. Viefhaus, DESY
P05	Micro- and nano-tomography / imaging	2 m U29	5 - 50 keV	side	A. Haibel, GKSS
P06	Micro/nano-spectroscopy / fluorescence	2 m U32	2.4 - 100 keV	straight	G. Falkenberg, DESY
P07	High energy materials science and diffraction	4 m U19	50 - 250 keV		N. Schell, GKSS/DESY
P08	High resolution diffraction	2 m U29	5.4 - 30 keV	top	O. Seeck, DESY
P09	Resonant scattering / diffraction	2 m U32	2.4 - 50 keV	straight	J. Strempfer, DESY
P10	Coherence applications	5 m U29	4 - 25 keV		M. Sprung, DESY
P11	MX-diffraction / biological imaging	2 m U32	2.4 -33 keV	side	A. Meents; MPI, HGF, DESY
P12	BioSAXS	2 m U29	4 - 20 keV	straight	M. Rößle, EMBL/GKSS
P13	Macro molecular crystallography I	2 m U29	4 - 17 keV	side	M. Cianci, EMBL
P14	Macro molecular crystallography II	2 m U29	7 - 35 keV	straight	G. Bourenkov, EMBL

high beta section	142x5 µm
low beta section	35x6 µm

HAXPES at PETRA III

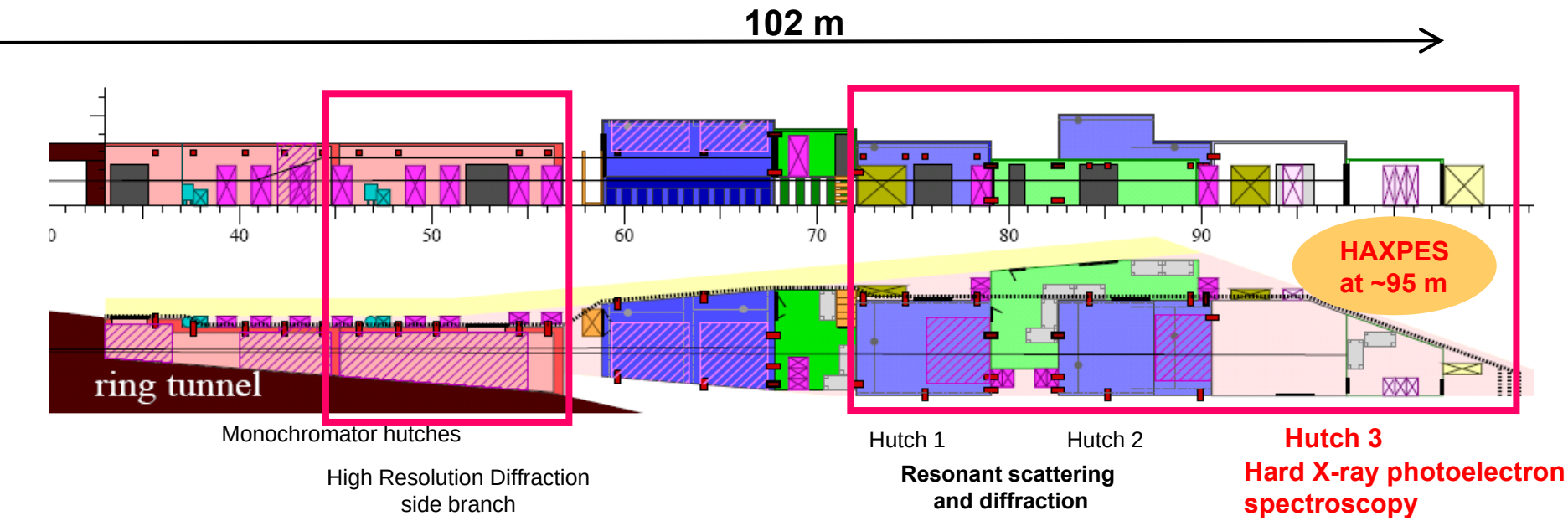

P09 "Resonant X-ray scattering"

Photons: - 2.4 – 50 keV

hutch 1: - high-precision Psi-diffractometer
- beam size at sample position 140 x 50 μm^2 (FWHM)

hutch 2: - heavy load diffractometer with 15 T cryomagnet / 60 T pulsed field option

hutch 3: - Hard X-ray photoelectron spectroscopy

HAXPES at PETRA III

Claudia Felser
(Chemistry Dept. Univ. Mainz)

Ralph Claessen
(Physics Dept. Univ. Würzburg)

Wolfgang Drube
(DESY)

Bulk electronic structure with high energy resolution:

- Complex correlated and magnetic materials
- Embedded interfaces and nanostructures
- Multifunctional composite materials
- Magnetic devices

Additional funding from BMBF
(federal ministry of research)

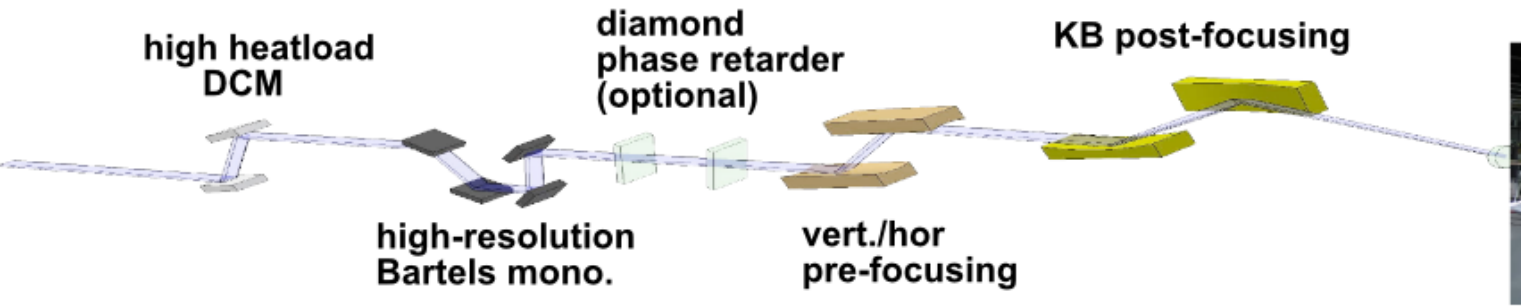

SPECS Phoibos 225
electron analyzer
(Univ. Mainz, operating)

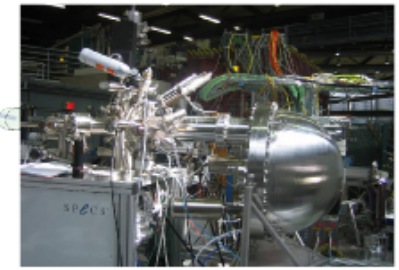

HAXPES at PETRA III

Schematic beamline layout

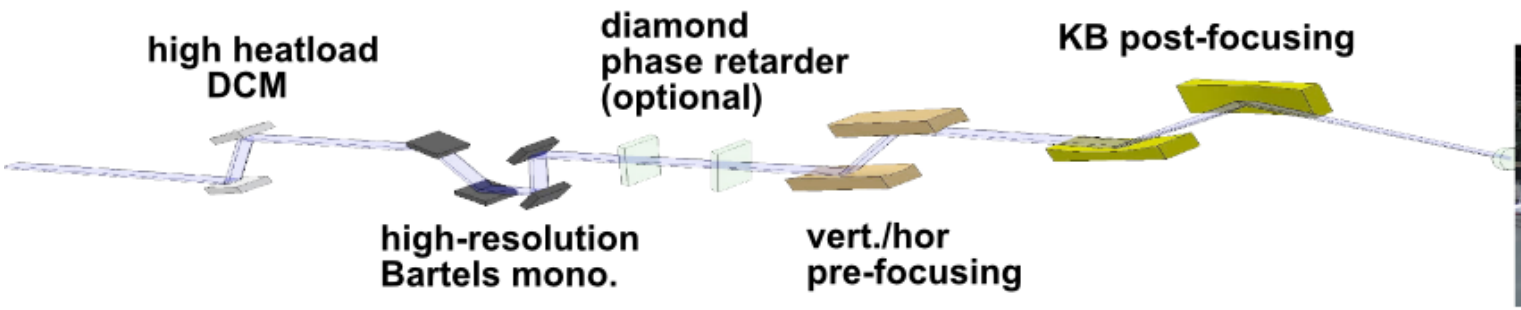

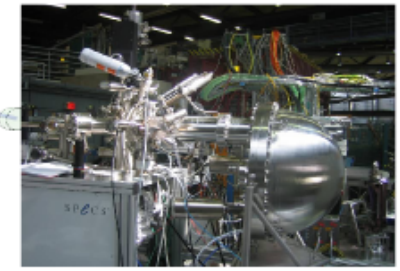

SPECS Phoibos 225
electron analyzer
(Univ. Mainz, operating)

Photons:

spectroscopy undulator (high-ß source) 2.4 - 15 keV
variable circular + linear polarization (phase retarder)
high-res. 4-crystal post-mono (down to 10 meV)
95 m source to sample distance
KB focus down to ~ 1µm x 1µm

Electrons:

SPECS Phoibos 225 analyzer, up to 15 keV
resolution down to ~15 meV (at ~10-15 keV)
Optional: spin analysis

P09 undulator

1st harm. 2.4 – 10 keV
3rd harm. 9 – 25 keV

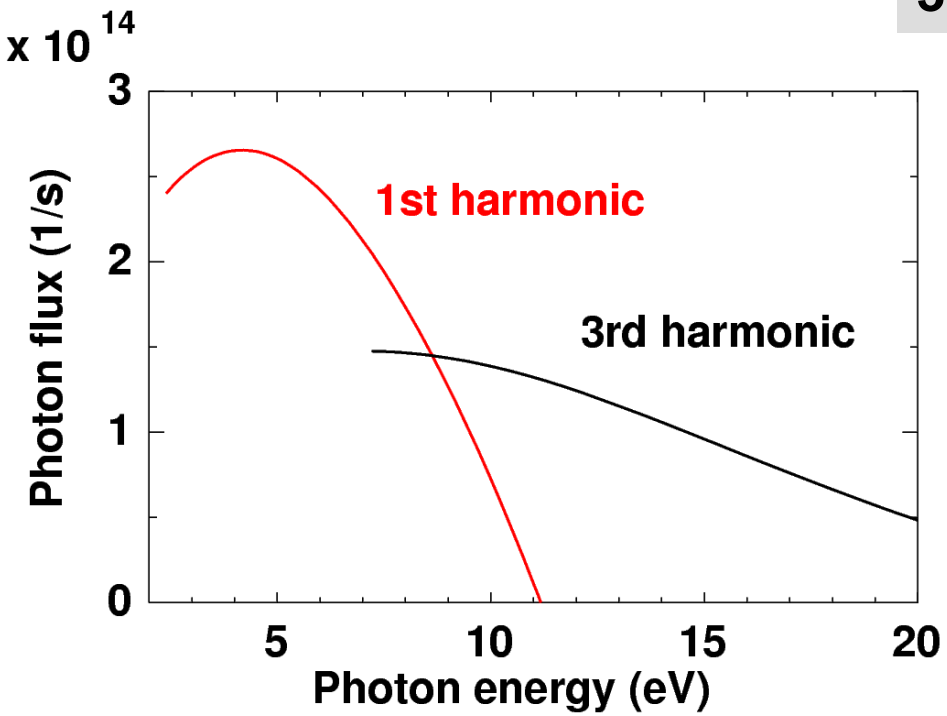

flux through 1 x 2 mm² at 35 m
(1st mirror position) into 10^{-4} BW

PETRA III P09 high heatload DCM

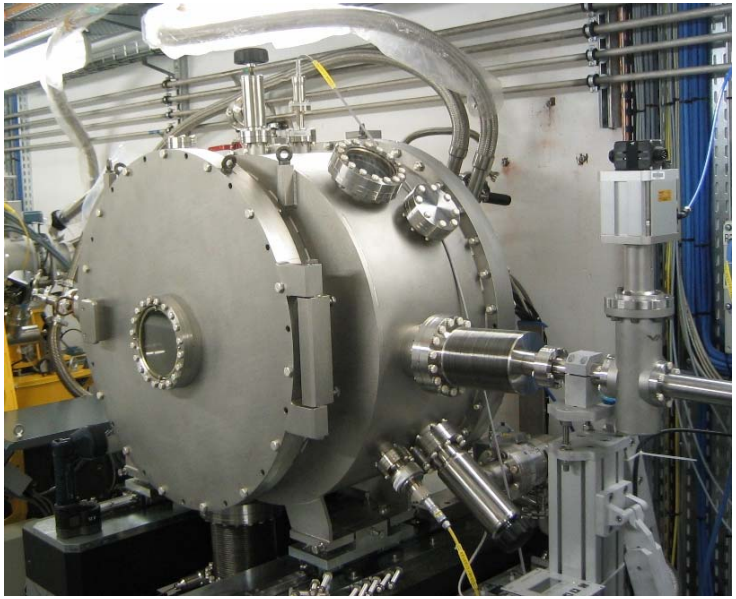

prototype test (2008) at ESRF ID6

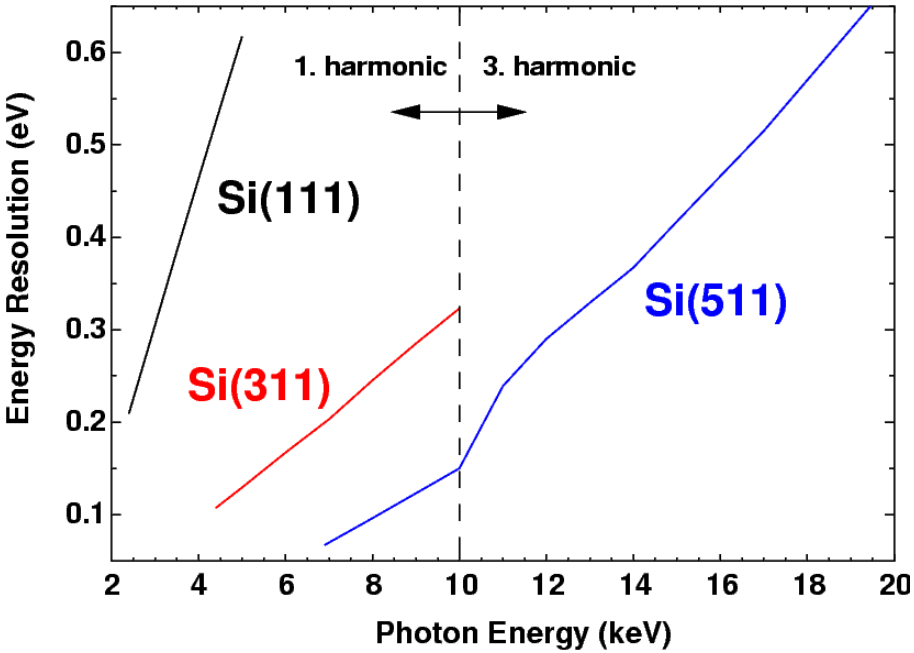

Medium resolution: 100 – 300 meV
readily available from Si(311) HHL DCM
4.2 - 10keV with full tunability
PETRA high-β source matches Si(311)

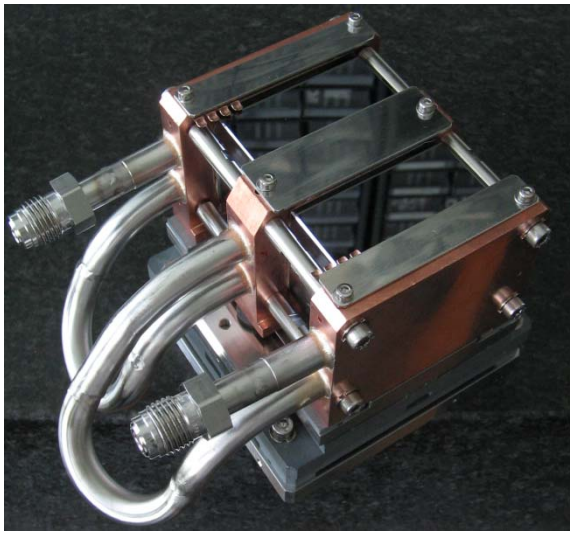

Si(111) / Si(311) standard crystal set

P09 HAXPES post-monochromator

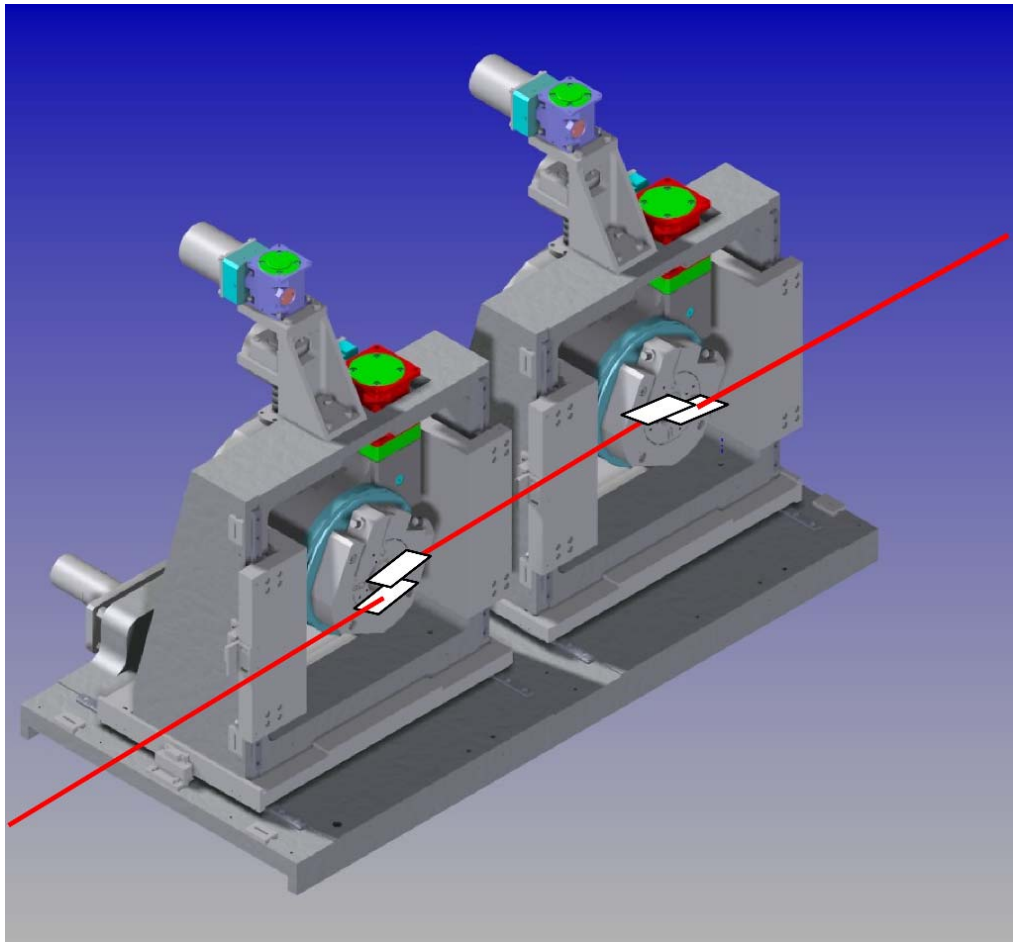

ESRF ID32 design, modified for PETRA III P09 commissioning fall 2009

High resolution: < 100 meV
achieved with high-resolution post-monochromator
("+- - +" Bartels-type, zero offset)
~ 50-10 meV in the range
6-15 keV with flux > 1×10^{11} 1/s

some energy tunability
(crystal design not fixed yet)

Variable circular and linear polarization

Dual-stage diamond transmission phase retarder

Diamond (111) phase plates

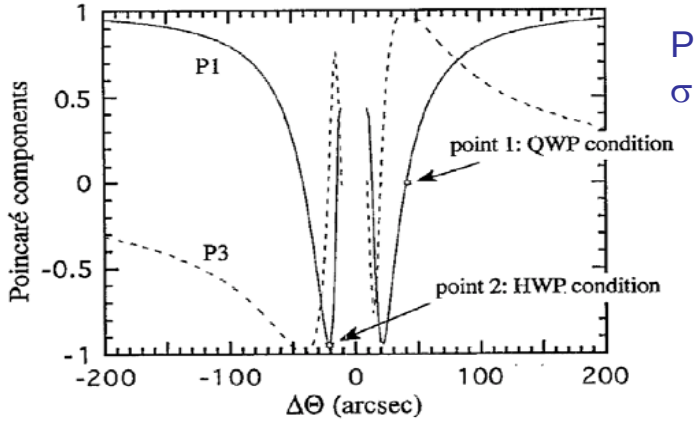

Phase difference between σ and π-component:

$$\Phi \sim \frac{t}{\Delta\Theta}$$

APS design

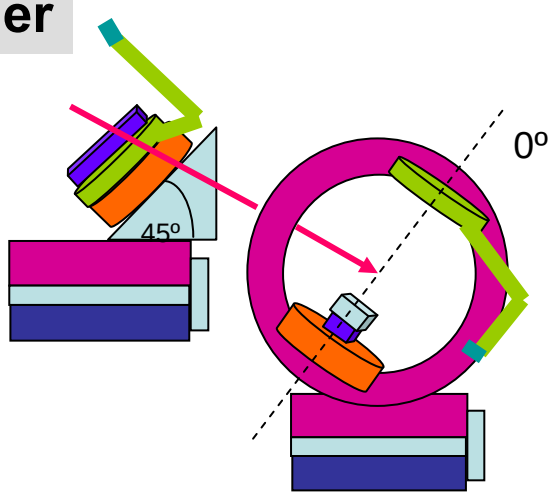

commissioning fall 2009

Circular polarization (XMCD, spin detection ...)

- → **Fast left-right switching, 20-40 Hz**
- → **Compensation of intensity differences by 1/8 phase plates in series (Lang et al., APS Annual Report 2005)**

Variable linear polarization:

- → **Half wave plate condition**
- → **Continuous rotation of linear polarization with two QWP in series**

Relevant for HAXPES:

- → **usable from ~4.5 to ~10 keV (diamonds with different thicknesses)**
- → **overall transmission ~30-40%**

HAXPES hutches and instrumentation

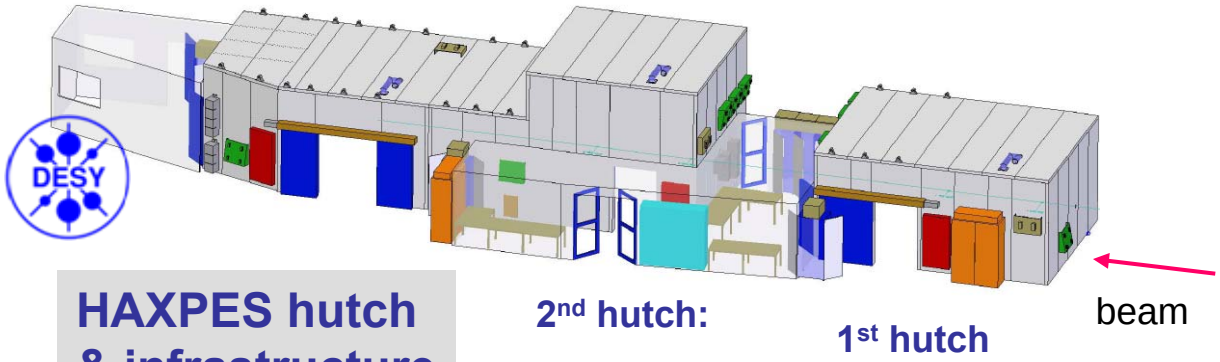

incl. BMBF funding for
- high res. mono
- KB post focusing

JOHANNES GUTENBERG UNIVERSITÄT MAINZ

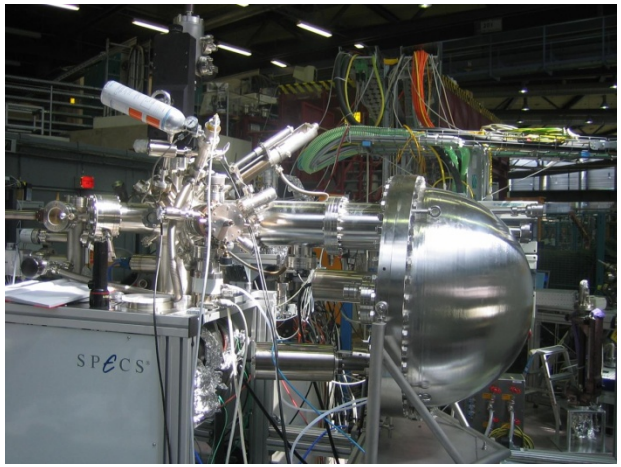

- SPECS *Phoibos 225 HV*
- up to 15 keV kinetic energy
- combined delayline, micromott-Spin detector
- Resolution ~15 meV in HAXPES-Mode

Julius-Maximilians-UNIVERSITÄT WÜRZBURG

- OMICRON *XPD-manipulator,*
- motorized 5-axis manipulator
- integrated LHe-cryostat (T < 18K),

HAXPES endstation at PETRA III

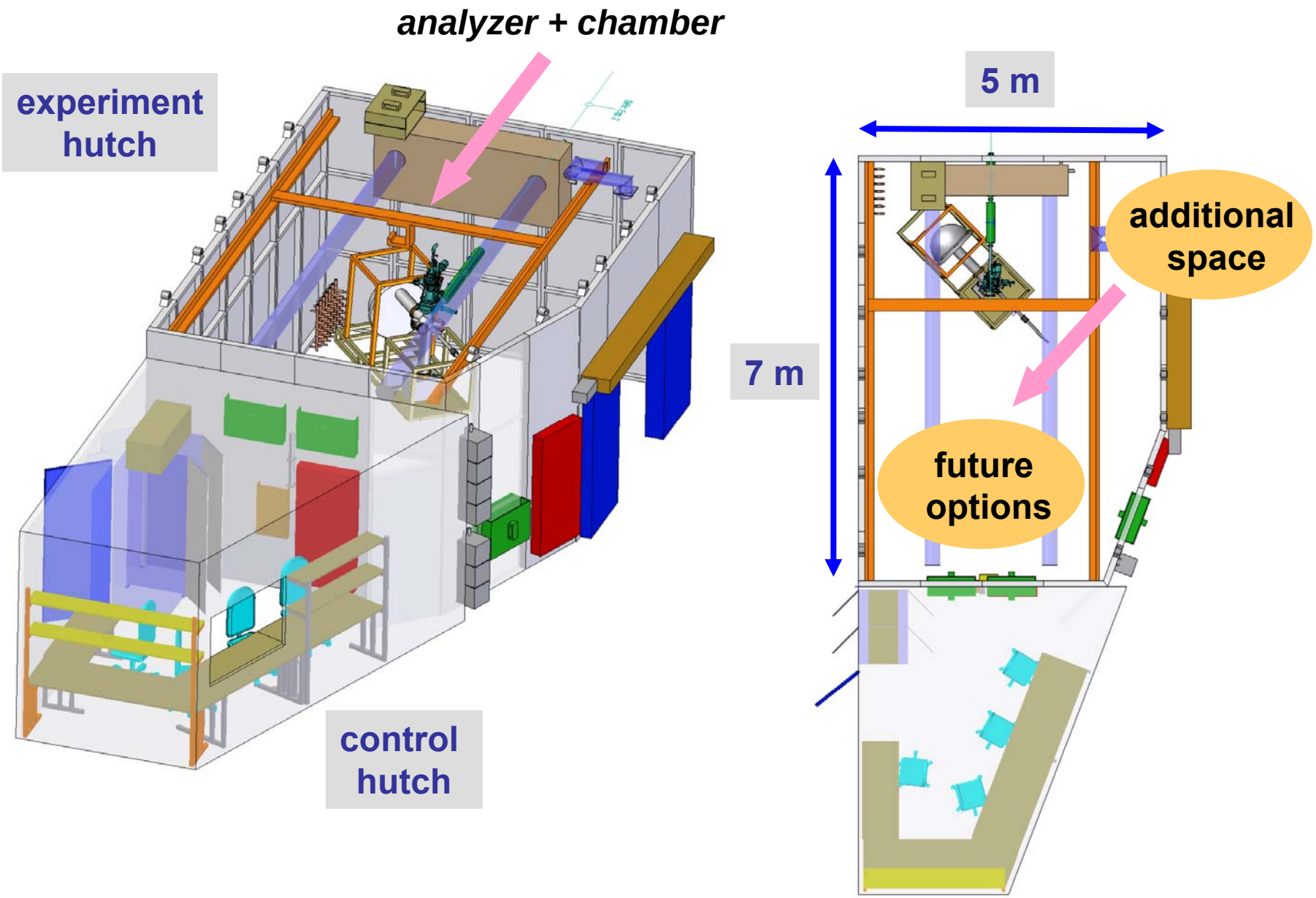

PETRA III: current status (May 2009)

PETRA III: current status (May 2009)

PETRA III: current status (May 2009)

PETRA III: current status (May 2009)

PETRA III: current status (May 2009)

HAXPES hutch at P09

PETRA III: current status (May 2009)

HAXPES control hutch at P09

PETRA III: current status (May 2009)

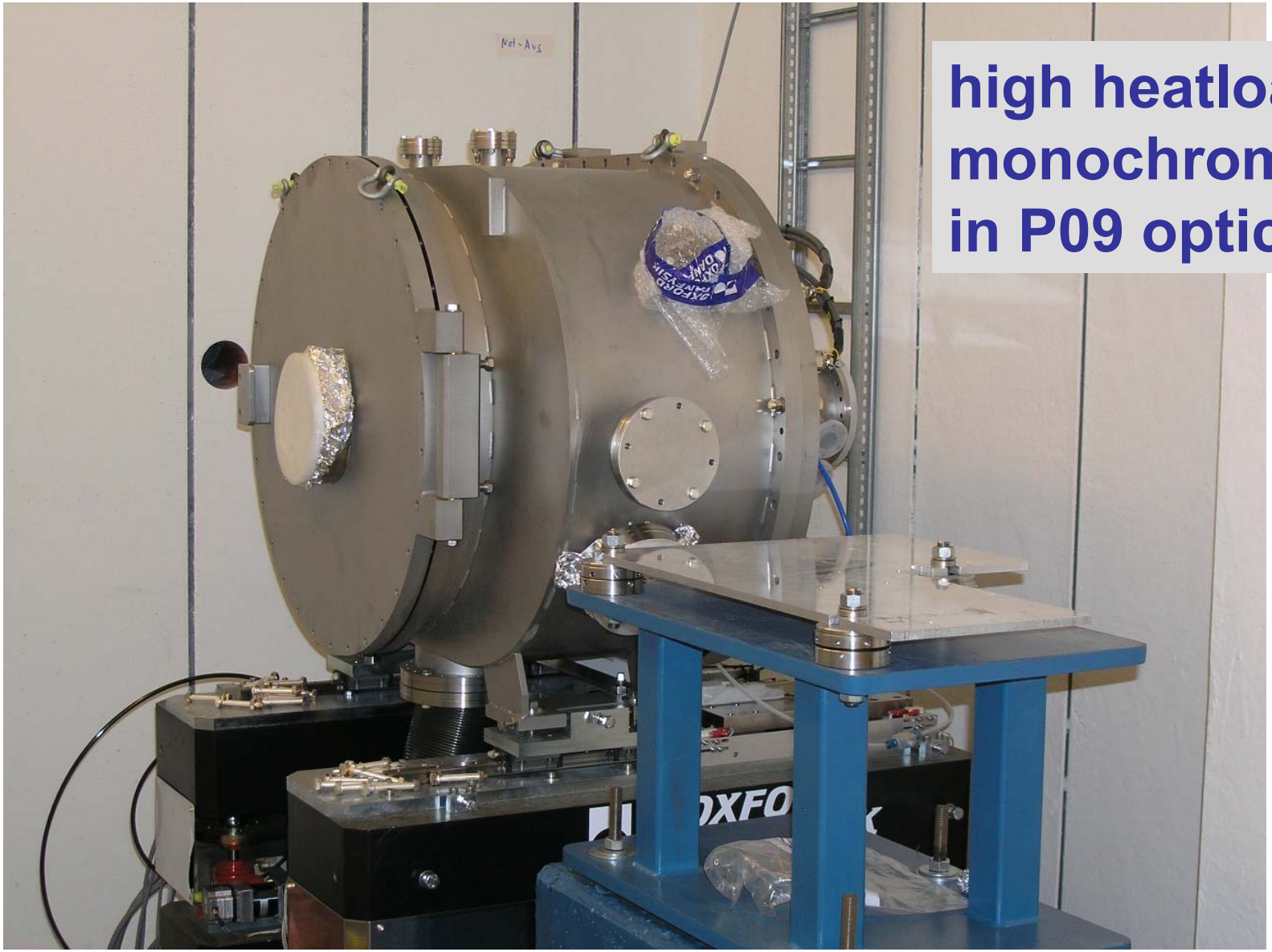

high heatload monochromator in P09 optics hutch

April 13: first positron beam stored in PETRA III

Beam was stored on April 13 (one bunch with 20 μA i.e. about 10^9 e+)
RF – phase right and orbit empirically corrected in the new octant

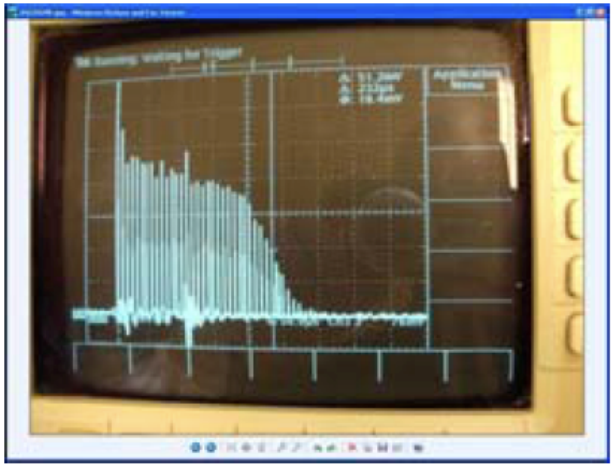

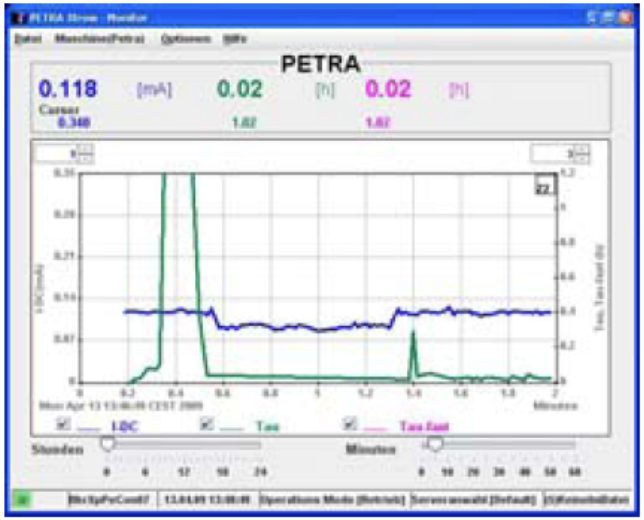

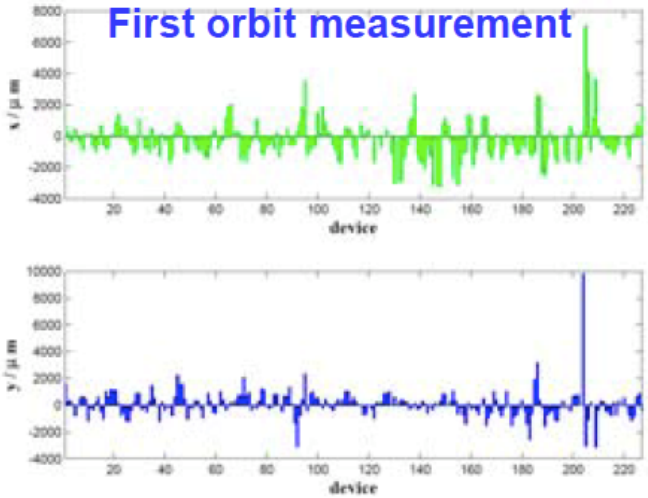

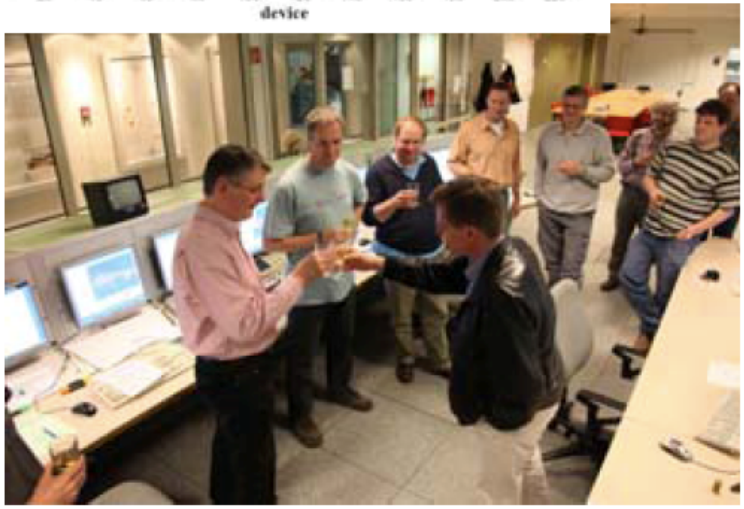

April 30: first undulator beam in P09 optics hutch

First light on April 30:

- Undulator PU 9 (OL 142m)
- Single bunch 0.5 mA
- Gap closed to 10 mm (foreseen 9.5)
- No effect on machine (orbit / tune)
- Beam centred with horizontal and vertical Bumps
- Power up to 8W

Screen monitor at 17.5 m

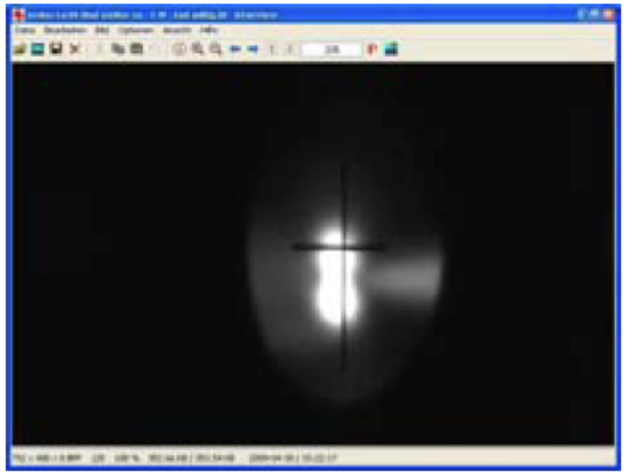

Undulator gap open

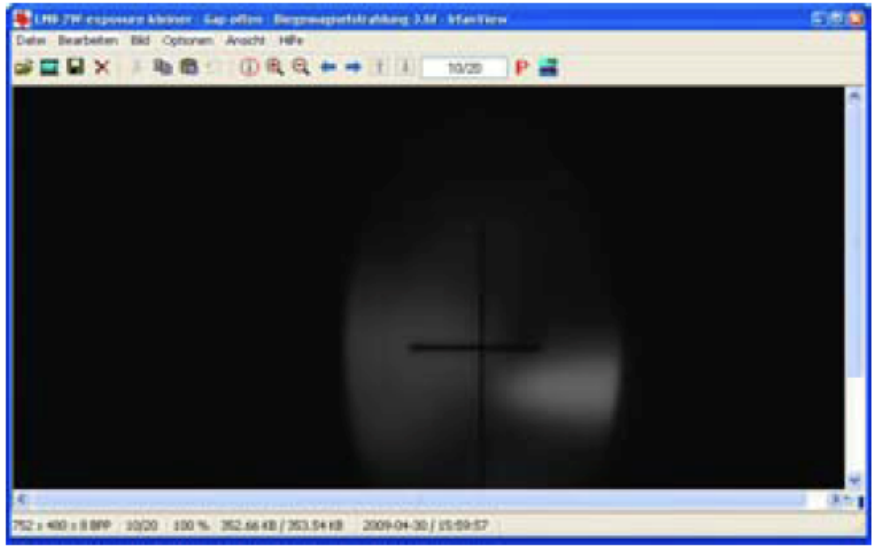

Screen monitor at 28m

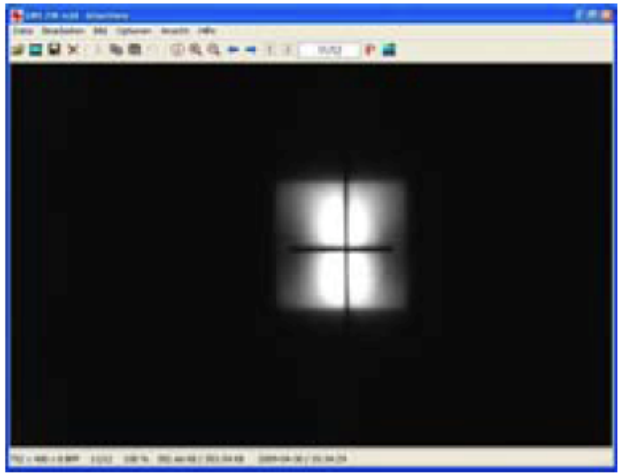

HAXPES instrument status

1st commissioning beamtime at DORIS III (wiggler BW2) in Feb/March 2009

additional modifications, tests, upgrades ongoing

high-precision instrument platform testing (May 15)

first beam on a sample at PETRA ~July 2009

DESY photon science activities by ~2014

Very near future: summer 2009

Thank you !